Barite ($BaSO_4$) biomineralization at Flybye Springs, a cold sulphur spring system in Canada's Northwest Territories

Sandy M. Bonny and Brian Jones

Abstract: The Flybye Springs, Northwest Territories, consist of 10 active vents and numerous small seeps that discharge sulphide- and barium-rich spring waters at an average temperature 8.5 °C. Oxidation of sulphide to sulphate drives precipitation of stellate and platy barite microcrystals in the proximal flow paths. Downstream, and in vent- and tributary-fed ponds, barite is precipitated among streamer and mat forming colonies of sulphur-tolerant microbes, including *Thiothrix*, *Beggiatoa*, *Thioploca*, *Chromatium*, *Oscillatoria*, fungi (dominantly *Penicillium*), and unicellular sulphate reducing bacteria. These microbes mediate barite saturation by adjusting redox gradients and via passive adsorption of barium ions to cell surfaces and extracellular polymeric substances. Passive biomineralization produces barite laminae in floating microbial mats, nanometric coatings, and micrometric encrustations around microbial cells and filaments, and local permineralization of *Thiothrix*, *Beggiatoa*, and *Oscillatoria* outer cell walls. Intracellular barium enrichment and (or) metabolic sulphur oxidation may be important to "active biomineralization" that produces nanometric barite globules on the tips of fungal hyphae, barite-filled cell cavities in *Beggiatoa* and *Thiothrix*, and baritized sulphur globules. Degradation of biomineralized cells generates detrital "microfossils," including barite tunnels, layered cylinders, solid cylindrical grains and chains of barite beads. The diversity of inorganic and biomineralized barite in the Flybye Springs flow path highlights the influence of ambient chemistry, microbial metabolism, and cellular structure on barite solubility and on the taphonomy of microfossils preserved in barite.

Résumé : Les sources Flybye, aux Territoires du Nord-Ouest, comprennent 10 évents actifs et de nombreuses petites résurgences qui déchargent des eaux de source riches en sulfures et en baryum à une température moyenne de 8,5 °C. L'oxydation des sulfures en sulfates cause la précipitation de microcristaux de barytine, de formes étoilées et lamellaires, dans les chemins de coulée proximaux. Vers l'aval, et dans des étangs alimentés par les évents et les tributaires, la barytine est précipitée parmi des colonies de microbes tolérant le soufre et qui produisent des filaments et des mattes; ces microbes comprennent *Thiothrix*, *Beggiatoa*, *Thioploca*, *Chromatium*, *Oscillatoria*, des champignons (principalement *Penicillium*) et des bactéries unicellulaires sulfatoréductrices. Ces microbes atténuent le saturation de la barytine en régulant les gradients redox et par l'adsorption passive d'ions baryum sur la surface de cellules et sur des substances polymères extracellulaires. La biominéralisation passive produit des lames de barytine dans les mattes microbiennes flottantes, des revêtements d'échelle nanométrique et des incrustations d'échelle micrométrique autour des cellules et des filaments microbiens ainsi que la pétrification locale des parois externes des cellules de *Thiothrix*, de *Beggiatoa* et d'*Osciallatoria*. L'enrichissement intracellulaire en baryum et (ou) l'oxydation métabolique du soufre pourraient être importants pour la « biominéralisation active » qui produit des globules de barytine d'échelle nanométrique aux extrémités des hyphes fongiques, des cavités cellulaires remplies de barytine dans *Beggiatoa* et *Thiothrix*, ainsi que des globules de soufre « barityniséés. » La dégradation des cellules biominéralisées génère des « microfossiles » détritiques qui comprennent des tunnels de barytine, des cylindres stratifiés, des grains solides en forme de cylindres et des chaînes de particules de barytine. La diversité de la barytine inorganique et biominéralisée dans le chemin d'écoulement des sources Flybye montre l'influence de la chimie ambiante, du métabolisme microbien et de la structure cellulaire sur la solubilité de la barytine et la taphonomie des microfossiles préservés dans la barytine.

[Traduit par la Rédaction]

Received 6 June 2006. Accepted 23 November 2006. Published on the NRC Research Press Web site at http://cjes.nrc.ca on 21 July 2007.

B. Chatterton served as Acting Editor for this paper.

Paper handled by Associate Editor C. Hillaire-Marcel.

S.M. Bonny[1] and B. Jones. Department of Earth & Atmospheric Sciences, 1–26 Earth Science Building, University of Alberta, Edmonton, AB T6G 2E3, Canada.

[1]Corresponding author (email addresses: bonny@ualberta.ca).

 doi:10.1139/E06-126

Introduction

Mineral springs that precipitate calcite, aragonite, silica, and iron oxides in microbially colonized flow paths are globally abundant. Research at these springs has provided insight into the controls on mineral solubility, crystallography, and microfossil preservation (Walter and Des Marais 1993; Westall 1999; Jones et al. 2000; Konhauser et al. 2003), improving the interpretative potential of chemical sediments in the geologic record (e.g., Arp et al. 2001; Kaufman and Xiao 2003). In contrast, springs that precipitate barite ($BaSO_4$) as a dominant mineral phase are rare (Cadigan and Felmlee 1977; Sasaki and Minato 1982; Younger 1986), and the influence of microbes on barite precipitation has only recently come under investigation (Senko et al. 2004).

The Flybye Springs in Canada's Northwest Territories are unique as the only known location where barite precipitates as a dominant mineral phase from cold spring water. The Flybye spring water is barium-rich (up to 12 ppm), contains high levels of dissolved sulphide, and supports a microbial community dominated by sulphur-oxidizing bacteria, sulphur-tolerant cyanobacteria, and fungi. These microbes assert microenvironmental influence on redox and ionic concentration gradients and thus mediate barite solubility in, on, and around microbial mats, cells, and intracellular inclusions. Barite precipitated through microbial mediation, or biomineralization, at Flybye Springs commonly produces microfossils that preserve the dimensions of microbial cells and cellular inclusions. Although the geochemical cycling of barium is strongly linked to organic productivity (Bertram and Cohen 1997; Ganeshram et al. 2003), and the influence of sulphur-metabolizing microbes on barite saturation gradients is well established (e.g., Baldi et al. 1996; Senko et al. 2004), the textural products of barite biomineralization have not been documented outside of laboratory experiments (e.g., Sakorn et al. 2002; Gonzalez-Munoz et al. 2003).

This paper uses a combined geochemical and microscopic approach to describe the unique physiochemical and microbiological characteristics of the Flybye Springs flow path that combine to facilitate what is, to the best knowledge of the authors, the first account of "natural" barite biomineralization and its microtextural artefacts.

Study site

The Flybye Springs sit at a southwesterly dipping contact between massive Devonian limestone and black, pyritic shale (Cecile 2000) exposed on the north side of a terraced valley between the Selwyn and Mackenzie mountain ranges in the Sahtu Region of Canada's Northwest Territories (Fig. 1A). There are numerous mineral springs in the area (Cecile 2000), but the Flybye Springs are the only ones known to precipitate barite as a dominant mineral phase. Barium in the Flybye spring water is thought to be derived from dissolution of barite microcrystals and barium-enriched feldspars dispersed in Paleozoic marine aquifer strata (Cecile et al. 1984; Orberger et al. 2005).

The Flybye spring water emerges through a sparsely vegetated crescent-shaped mound, 200 m^2 in area and up to 5 m high, which is composed of relict barite tufa formed by past activity at the springs. There are ten active spring vents and numerous small seeps concentrated on the southeastern side of the mound, and spring water flows downhill towards a mud wallow frequented by caribou and other wildlife (Fig. 1B). This study focuses on microbes and mineral precipitates found in the flow paths of the four largest spring vents, D1–D4 (Fig. 1C). Located just south of the Arctic Circle, the Flybye Springs experience harsh winters that precluded year-round observation of the field site—all data pertain to summer (July–August) conditions.

Methods and materials

Fieldwork

The pH, conductivity, and dissolved oxygen (DO) content of the Flybye spring water were measured across the spring site in July 2004 and August 2005 using a portable Accumet AP62 pH/mV meter and an Orion Model 1230 D.O./pH/mV probe. Water samples were collected from vents D1–D4 through a 0.45 μm pore size Fisherbrand water-testing membrane, and stored in sterile 250 mL Nalgene containers for isotopic and elemental analysis. $H_2S_{(g)}$ dissolved in the spring water was collected from the flow path beneath vent D1 by precipitation as CdS. Gases exsolving from a vent-fed pool below spring D2 were collected by filling a sterile Nalgene bottle with spring water, inverting it above a spring vent, and trapping the rising gas bubbles in the bottle.

Fresh mineral precipitates and microbial samples were collected in sufficient number to represent the textural and chromatic variability observed in the field. One half of each microbial sample was stored in spring water and the other was preserved in a 6:3:1 solution of water, 95% alcohol and formalin, with 5 mL of glycerol added per 100 mL. Twelve glass slides were placed in the proximal flow paths of vents D1–D4 in early July 2004. Despite careful flagging, only three slides were retrieved 10 months later, and two of these were fractured. Caribou hair, antlers, and hoof prints on the spring mound indicate that the site was disturbed repeatedly over the course of the year.

Laboratory analyses

Elemental spring water chemistry was determined by inductively coupled – mass spectrometry (ICP–MS) at the University of Saskatchewan, Saskatoon, Saskatchewan. Barium measured significantly lower than data reported by Cecile et al. (1984), prompting re-analysis of select samples by neutron activation analysis (NAA) at the University of Alberta's SLOWPOKE Facility (following Al-Jundi 2001). SOLMINEQ88 was used to evaluate the saturation state of the spring water with respect to relevant mineral phases. The gas sample was analyzed on a Finnigan Mat 252 mass spectrometer. The $\delta^{34}S$ of H_2S gas samples (precipitated as CdS and converted to AgS) and dissolved sulphate were determined by elemental analysis and isotope ratio mass spectrometry (EA–IRMS) at the University of Calgary Isotope Science Laboratory, Calgary, Alberta.

Mineral precipitates and retrieved glass slides were examined by petrographic microscope, X-ray diffraction (XRD), scanning electron microscopy (SEM), and energy dispersive X-ray analysis (EDX). SEM samples were desiccated, mounted on steel stubs with carbon tape, sputter coated with gold, and examined in secondary electron and backscattered

Fig. 1. Study area. (A) Location of the Flybye Springs. (B) Aerial view of Flybye Springs site. (C) Aerial view of boxed area in image B showing spring vents D1 to D4.

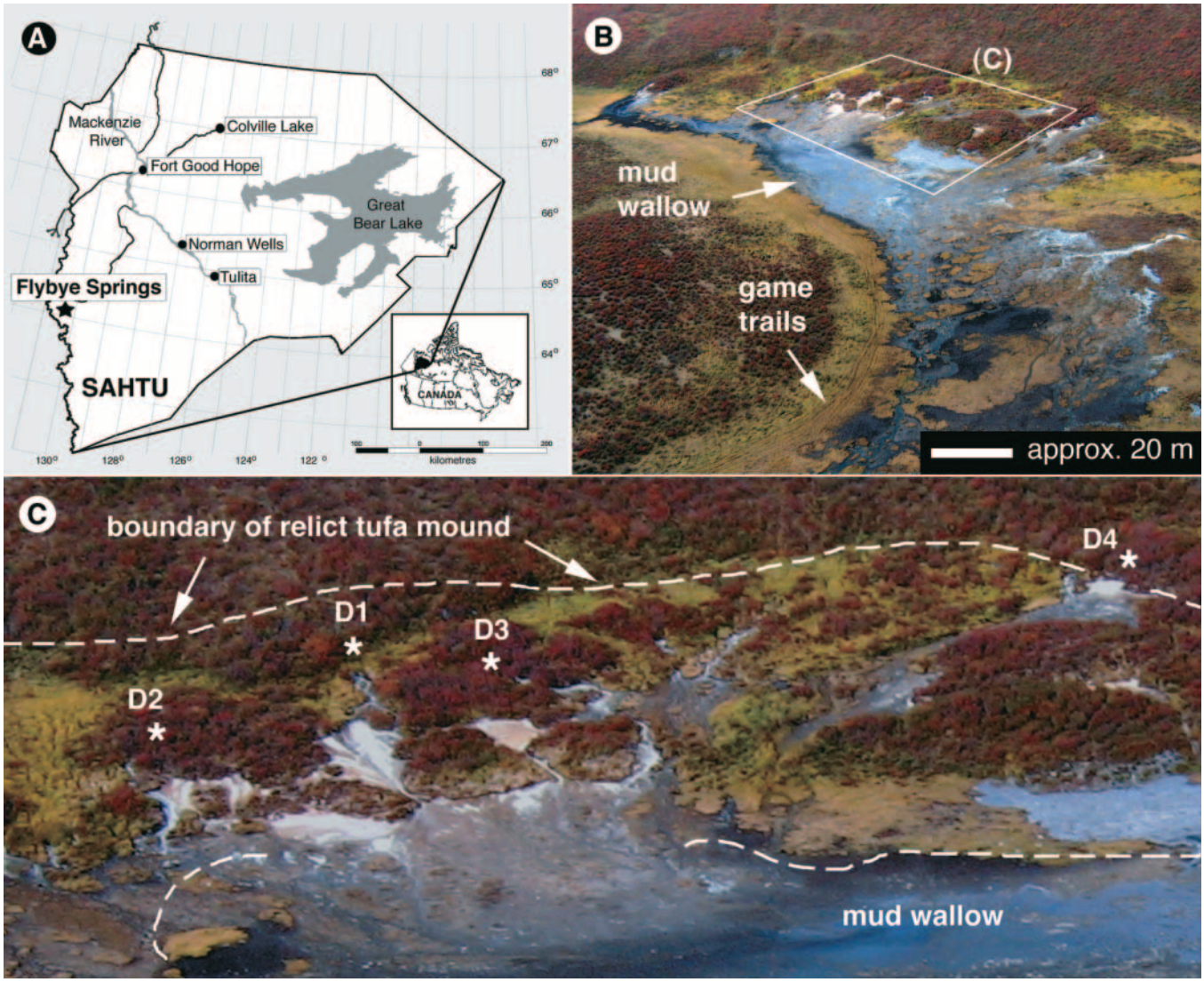

electron mode on a JEOL 6301 field emission scanning electron microscope at accelerating voltages of 5–30 kV. In backscattered electron SEM images, variations in atomic weight are reflected in image brightness—barium (with an atomic mass of 137.3) is very bright in contrast to increasingly dark sulphur (32.1), silicon (28.1), and organic material (~12.0).

Microbial samples were examined by light microscopy and SEM. Diatoms were identified to species level following Simonsen (1987). Where possible, soft-bodied microbes were identified by morphological criteria following Rippka et al. (1979), Reichenback (1981), Larkin and Strohl (1983), Schlegel and Bowien (1989), and Wher and Sheath (2003). The Flybye Springs filamentous microbes were identified to genus level with a high degree of confidence, but species assignments were not possible on the basis of morphology (cf. Douglas and Douglas 2001; Teske and Nelson 2005). A variety of submicron-sized unicellular microbes and actinomycetes were found in SEM, but as these forms are not volumetrically dominant or commonly mineralized, they were not identified. Powdered samples of microbes and detrital organic materials were also investigated by NAA to assess barium, radium, and strontium enrichment in biomass submerged in the Flybye spring water.

Results

Spring water physiochemistry

The Flybye spring water emerges with an average vent temperature of 8.5 °C and is heated by sunlight to 14 °C before entering the mud wallow. Water pH is circumneutral at the vents and increases downstream to a maximum value of 8.4. The spring water is anoxic to dysoxic on emergence, containing ≤0.54 mg/L dissolved oxygen, and exsolves malodorous H_2S gas.

Water emerging from vent D1 and nearby seeps has $\delta^{34}S_{sulphide}$ values ranging from 13.7‰–15.8‰, which are consistent with a sulphur source in Paleozoic marine strata (Cecile et al. 1984; Canfield 2001; Allen et al. 2002). The

$^{34}S_{sulphate}$ increases downstream in the D1 flow path, shifting from 17.3‰ at 1 m, to 19.0‰ by 5 m, then reverses the trend, dropping to a minimum of 14.7‰ in the distal flow path.

Flybye spring water becomes oxygenated (cf. van Everdingen 1972) an average distance of 8 m from its source; however, re-mixing with anoxic or dysoxic waters emerging from seeps in the lower mound complicate the dissolved oxygen profile of many spring water tributaries (Fig. 2). Stream-fed pools on the lower Flybye Spring mound are redox stratified, with anoxic, organic-rich bottom waters, and clear, oxygenated surface waters. Vent-fed pools on the upper mound are also redox stratified, with anoxic bottom waters and dysoxic surface waters (Fig 2).

Gas bubbles exsolving from a vent-fed pool were found to contain methane, propane, ethane, and iso- and normal butane, in a ratio consistent with a source in a medium maturity natural gas seep (K. Muehlenbachs, personal communication, 2006). The gas also contains carbon dioxide, which probably originated from CO_2 dissolved in spring water and microbial respiration in organic detritus accumulated in the pools.

The spring water contains high concentrations of sodium and chloride, and is anomalously enriched in barium relative to regional surface waters (Cecile et al. 1984) (Table 1**)**. Solutions are saturated with respect to mineral phases for which the saturation index (logarithm of the ion activity product divided by the solubility constant, or log IAP/K) is 0. Upon emergence, the Flybye spring water is near saturation with respect to calcite (–0.16 to 0.00), aragonite (–0.31 to –0.01), and chalcedony (–0.02 to 0.10), undersaturated with respect to witherite (–2.48 to –0.82), and supersaturated with respect to barite (0.99 to 2.32) (using SOLMINEQ88).

During the summer months, all inundated parts of the Flybye flow path are microbially colonized, and desiccated mat samples were found to be up to three times enriched in strontium compared with surrounding spring water, and contain up to 36.5 wt.% barium. This corresponds to roughly 14 wt.% barium in hydrated mats, or 24.8 wt.% barite if all mat-bound barium were precipitated with sulphate.

Spring biology

Microbes inhabit all inundated parts of the Flybye Springs mound. Good correlation was found among the macroscopic appearance of microbial colonies, their constituent microbial genera, and spring water physiochemistry (Table 2; Fig. 2). The flow paths of springs D1, D2, and D3 share a downstream progression of microbial genera (Fig. 2).

In proximal dysoxic flow paths, white fringes 1–3 cm long (Fig. 2A) composed of *Thiothrix* (Figs. 3A, 3B) are established within 1.5–2 m of most vents and seeps. In dysoxic eddies and pools downstream, filaments of *Beggiatoa* (Fig. 3C) are intertwined with *Thiothrix* in streamers up to 5 cm long, which also contain abundant mucus, or extracellular polysaccharides (EPS) (Fig. 2B).

Redox-stratified vent-fed ponds have tiered microbial communities (Fig. 2C). *Thioploca* (Figs. 3D, 3E) forms black-green, EPS-rich drapes with sulphur-reducing bacteria and *Chromatium* (Fig. 3F) in degrading organic detritus in anoxic bottom waters. Diatoms (including *Achnanthes minutissima*, *Achnanthes flexella*, *Cymbella microcephala*, and species of *Amphora* and *Navicula*), *Oscillatoria* (Figs. 3G–3I), and *Beggiatoa* cohabitate in green–brown microbial mats floating in dysoxic waters 3–10 cm below the surface of the ponds.

Ponds fed by spring water tributaries have oxygenated surface waters with floating bubbly, laminated green–orange mats (Fig. 2D). The top layer of these mats is dominated by cyanobacteria, including *Oscillatoria*, *Planktothrix*, and an *Anabaena*-like cyanobacterium that lacks heterocysts (Figs. 3I, 3J), and diatoms. Basal layers of mats contain patches of *Beggiatoa* filaments, degrading cyanobacteria, and *Chromatium*. Sulphur-reducing bacteria colonize detrital organics accumulated at the bottom of the ponds.

Substrates bordering spring water tributaries are commonly encrusted by yellow films composed of sulphur and fungal hyphae (Figs. 3K, 3L). Although it cannot be certain that samples were not contaminated after collection, SEM analysis of these films showed that they are dominated by *Penicillium* sp. *Thiothrix* filaments were found intertwined with fungal hyphae in several areas, which indicates that the fungi are endemic to the edges of the spring flow path. Fungal diversity may be limited by the high sulphur content of the spring water, which is inhibitory to many fungal species (Gadd 1993; Rajashekhar and Kaveriappa 2003).

Fungal hyphae are also present in organic detritus in the spring flow path. Beneath overhanging shrubbery, many "microbial" mats floating in vent- and stream-fed ponds contain up to 80% degrading leaves, by volume. The air-exposed surfaces of these "leafy mats" are heavily colonized by fungi. Submerged leafy mat surfaces are commonly magenta due to dense colonization by *Chromatium*.

Mineral precipitates

Glass slides left in the proximal flow paths for 10 months developed mineral encrustations 50–250 m thick, suggesting a very slow rate of mineral precipitation from spring water (Fig. 4A). Rocks, desiccating microbial mats and streamers, and detrital organics submerged in spring water tributaries, however, bear yellow films of elemental sulphur and yellow–grey mineral encrustations up to 5 mm thick (Fig. 4B). The yellow–grey crusts are composed of microbial cells and EPS, microcrystalline barite, amorphous silica in the form of diatom frustules and algal cysts, and elemental sulphur (Figs. 4C, 4D).

Sulphur is found as microcrystalline rhombic crystals and spherical globules (Fig. 4E). Crystalline elemental sulphur is a typical product of inorganic redox reactions in oxygenating spring water (Douglas and Douglas 2000). The spherical globules, however, are identical in size and shape to those produced by sulphur-metabolizing bacteria (Figs. 3B, 3C, 3F) and are most likely biogenic (cf. Douglas and Douglas 2001).

Barite is the most abundant and least soluble mineral precipitating from Flybye spring water. The Flybye barite is relatively pure, containing <0.3% calcium and <0.5% strontium, but is radioactive (up to 8 Sv/h, or three times background levels) due to co-precipitation of radium (Cecile et al. 1984).

Inorganic barite precipitation

The Flybye spring water is supersaturated with respect to barite with even slight oxidation of vent waters (Kharaka et al. 1988: SOLMINEQ88). Proximal to spring vents, barite precipitates in suspension as stellate microcrystals, 4–10 m in diameter (Fig. 5A); scalloped platy microcrystals, 0.5 m

Fig. 2. Schematic representation of flow path beneath vent D1. (A) Idealized profile of flow path below vent D1 showing physiochemical data and distribution of microbial communities. (B) Fringes of *Thiothrix*. (C) Streamers composed of *Thiothrix* and *Beggiatoa* filaments. (D) Tiered microbial mats in a vent-fed pond. (E) Bubbly microbial mat from stream-fed pond (pocket knife is 10 cm long).

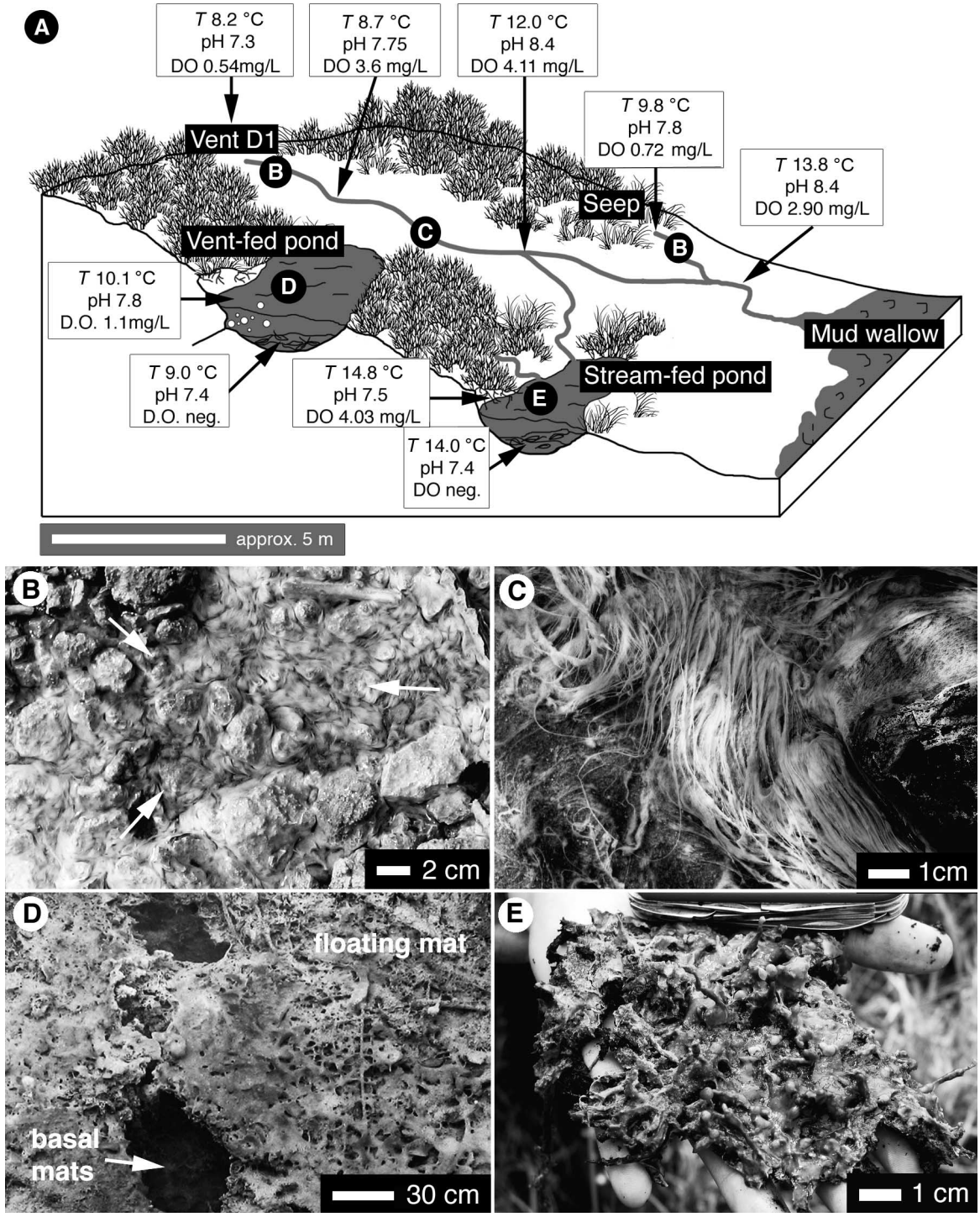

to 1 μm long, which are composed of subhedral platy microcrystals 200 nm wide (Figs. 5B, 5D); and intergrown tabular microcrystals 0.5–3 μm wide (Figs. 5C, 5D). These barite crystals accumulate among microbial mats and streamers bordering the flow paths, and continued crystal growth commonly envelops microbial cells or EPS strands (Figs. 5C, D). Microbial cells are also enveloped by balls of blocky barite microcrystals, up to 40 mm in diameter, found among porous clumps of detrital plant material and animal hair in proximal flow path tributaries (Figs. 5E, 5F). Spontaneous precipitation of barite from spring water ceases beyond ~5 m of most spring vents, and inorganic barite crystals are found only as scattered, presumably detrital, grains.

Table 1. Average chemical composition (in ppm) of Flybye Springs vent waters.

	Cecile et al. (1984)	ICP–MS (2004)	ICP–MS (2005)	NAA (2005)
Ca^{2}+	38	47	42	
Mg^{2}+	18	11.7	15.6	
Mn^{2}+				0.016
K+	3.3	2.6	3.2	
Na+	62	52.6	56.7	
Ba^{2}+	112[a]	0.57[b]	3.38	12
Sr^{2}+		0.02[b]	1.06	
Fe^{2}+	<0.025	0.08	0.007	
Pb^{2}+	0.013	0.018		
Cl^{-}	110	72.9	61	72.4
HCO_3^{2-}	245		192	
SO_4^{2-}	36	53.4	53.3	
NO_3^{-}			2.2	
UO_2	0.007	0.001		
SiO_2	7.4	4.9	3.7	
Ra (pCi/L)[c]	41.5 (1.5 Bq/L)			

Note: ICP–MS, inductively coupled plasma mass spectrometry; NAA, neutron activation analysis; data from Cecile et al. (1984) were generated by atomic adsorption mass spectrometry.

[a]May have been estimated from charge balance calculations rather than measured directly.

[b]Anomalously low values may reflect difficulties with the ICP–MS method for measuring these elements (cf. Al-Jundi 2001).

[c]1 pCi = 37 mBq.

Barite laminae in microbial mats

Mats in the proximal flow path entrap randomly distributed detrital barite microcrystals, but elsewhere on the spring mound, most mat-bound barite is concentrated in narrow laminae. Mats floating in spring water ponds commonly contain one or more barite laminae ≤10 μm thick (Figs. 6A, 6B). These laminae are sandwiched between lower *Beggiatoa*-rich and upper *Oscillatoria* – diatom-rich mat layers in dysoxic, vent-fed ponds, and between lower *Beggiatoa*-rich and upper *Oscillatoria–Anabaena (?)* – diatom-rich layers in surface oxygenated, stream-fed ponds (Figs. 6C, 6D). The barite laminae are composed of tightly packed anhedral to subhedral granular microcrystalline barite surrounded by EPS with few to no visible microbial cells (Figs. 6C, 6D).

"Leafy" microbial mats contain distinct barite laminae localized beneath the cuticular layers of degrading leaves. These laminae are composed of loosely packed composite barite spherules 0.8 to 5.0 μm in diameter (Fig. 6E). There is a gradational change in the habit of the composite microcrystals with spherule size: spherules ≤1 μm are composed of radially arranged anhedral barite rods (Fig. 6F); intermediate-sized spherules are have an outer layer of subhedral platy crystals ≤100 nm long (Fig. 6G); and large spherules are coated by subhedral plates that are up to 0.5 μm long (Fig 6E).

Barite coated and encrusted microbes

Barite is found coating the outer surfaces of microbes of diverse genera throughout the Flybye spring system. Initial barite precipitation involves the deposition of globules of barite, <100 nm in diameter, on outer cell surfaces. Early globule precipitation is spatially specific in fungi, with globules concentrated at hyphal tips (Fig. 7A), but it appears random in other microbial groups (Fig. 7B). Progressive globule precipitation forms cell-encompassing coatings (Figs. 7C, 7D).

Globular barite coatings are common on *Thioploca* bundles growing in anoxic ponds, where they adhere to the exterior of *Thioploca*'s thick EPS sheath (Figs. 7D, 7E), and are basal to secondary encrustations. Unicellular bacteria, most likely sulphate-reducing bacteria (SRB), attached to the *Thioploca* sheaths are enveloped by these barite encrustations and preserved as ovoid molds (Fig. 7F).

Secondary encrustations can triple the diameter of coated microbes (Figs. 8A, 8B). They are composed of subhedral to euhedral platy barite crystals that precipitate in situ (Fig. 8C) and (or) detrital grains trapped by EPS films (Fig. 8D). Fragmentation of coated and encrusted microbial filaments generates tunnel-shaped detrital grains (Fig. 8D).

Barite-permineralized cell walls

The outer cell layers of *Thiothrix* and *Beggiatoa* growing as streamers in flow path tributaries, and *Beggiatoa* and *Oscillatoria* in the upper layers of mats floating in vent-fed ponds, are commonly impregnated, rather than coated, by nanometric barite globules (Figs. 9A–9C). Permineralized cell walls are basal to secondary encrustations of anhedral and subhedral barite microcrystals in many specimens (Figs. 9D–9F). Degradation of the cell contents following permineralization of the cell wall creates tunnel-shaped grains that, most commonly, are not only externally encrusted, but also filled by barite microcrystals (Figs. 9D, 9E). Fragmentation of these microfossils generates three-layered detrital grains (Fig. 9F).

Intracellular barite precipitation

A distinct mode of baritization was found in *Beggiatoa* and *Thiothrix* filaments growing near the top of a glass slide ~4 m from vent D2, and in *Beggiatoa* filaments from the bottom layer of mats floating in stream-fed ponds. These fil-

Table 2. Morphological and environmental details of the dominant microbial genera at the Flybye Springs**.**

Genus	Morphology	ISD	ST	Habitat	Flybye field appearance
Sulphur-oxidizing bacteria					
Thiothrix	Colourless cylindrical filaments; 1–2 μm wide; septa every 0.5–1 μm; unsheathed; occur in rosettes; adhere to filaments of *Beggiatoa*	Yes	Yes	Flowing dysoxic water	White fringes; streamers
Beggiatoa	Colourless cylindrical filaments; 3–5 μm wide; septae every 1–2 μm; unsheathed; occur singly; form hormogonia; gliding movement	Yes	Yes	Oxic–anoxic interface, low current conditions	Streamers; basal layers of floating mats; rarely top layers of floating mats
Thioploca	Up to 15 *Beggiatoa*-like filaments within a common sheath up to 20 μm in diameter; sheath has sub-regular constrictions and in some places longitudinal wrinkles; macroscopic green-blue colour	Yes	Yes	Bottom of dysoxic–anoxic lakes, ponds, and springs with elevated sulphide	Stringy drapes among organic detritus at the base of vent-fed ponds
Purple sulphur bacteria					
Chromatium	Motile; oval to bean shaped cells 1–3 μm long; pink in light microscope	Yes	Yes	In photic zone with hydrogen sulphide and organic carbon	Magenta patches on “leafy mats”; mid-lower layers of floating mats
Cyanobacteria					
Oscillatoria	Olive-green filaments; 5 μm wide; septa every 1 μm (or less); unsheathed; non-refractory internal granules; form hormogonia by necrotic cell development; gliding movement	No	Yes	Flowing or stagnant oxygenated to dysoxic water, wide chemical and thermal tolerance	Abundant in orange–green top-mid layers of floating mats
Planktothrix	Green filaments; 4–5 μm wide; septa every 1.5 μm; slightly constricted at cross walls; unsheathed; slightly expanded terminal cells	No	No	Cool to warm freshwater lakes and ponds	Top green layer of mats floating in stream-fed ponds
Anabaena (?)	Blue-green filaments; 3 μm wide; septa every ~4 μm; deep constrictions at cross walls; no heterocysts observed in filaments from Flybye Springs	No	No	Cool to warm freshwater lakes, ponds, and streams	Top green layer of mats floating in stream-fed ponds; mud wallow hoof prints

Note: ISD, intracellular sulphur deposition; ST, sulphide tolerant (after Rippka et al. 1979; Reichenback 1981; Larkin and Strohl 1983; Schlegel and Bowien 1989; Kojima et al. 2003; Wher and Sheath 2003; Teske and Nelson 2005).

Fig. 3. Light microscope and SEM images of microbes from Flybye Springs. (A) Rosettes of *Thiothrix*. (B) *Thiothrix* filaments with internal sulphur globules. (C) *Beggiatoa* filaments with internal sulphur globules. (D) Ensheathed *Thioploca* filament bundles. (E) Detail view of *Thioploca* bundle with deep sheath constriction points (arrows). (F) *Chromatium* with internal sulphur globules. (G) Filament of *Oscillatoria* with necrotic cells (arrows). (H) Filaments of *Oscillatoria* (**O**), with nonrefractory granular inclusions and *Beggiatoa* (B) with refractory sulphur globules. (I) Aligned filaments of *Oscillatoria* (**O**) and *Planktothrix* (**P**). (J) *Anabaena* (?) (A) filaments and a diatom (**D**). (K) Branching fungal hyphae among elemental sulphur rhombs and beads. (L) Detail of *Penicillium* conidiophores.

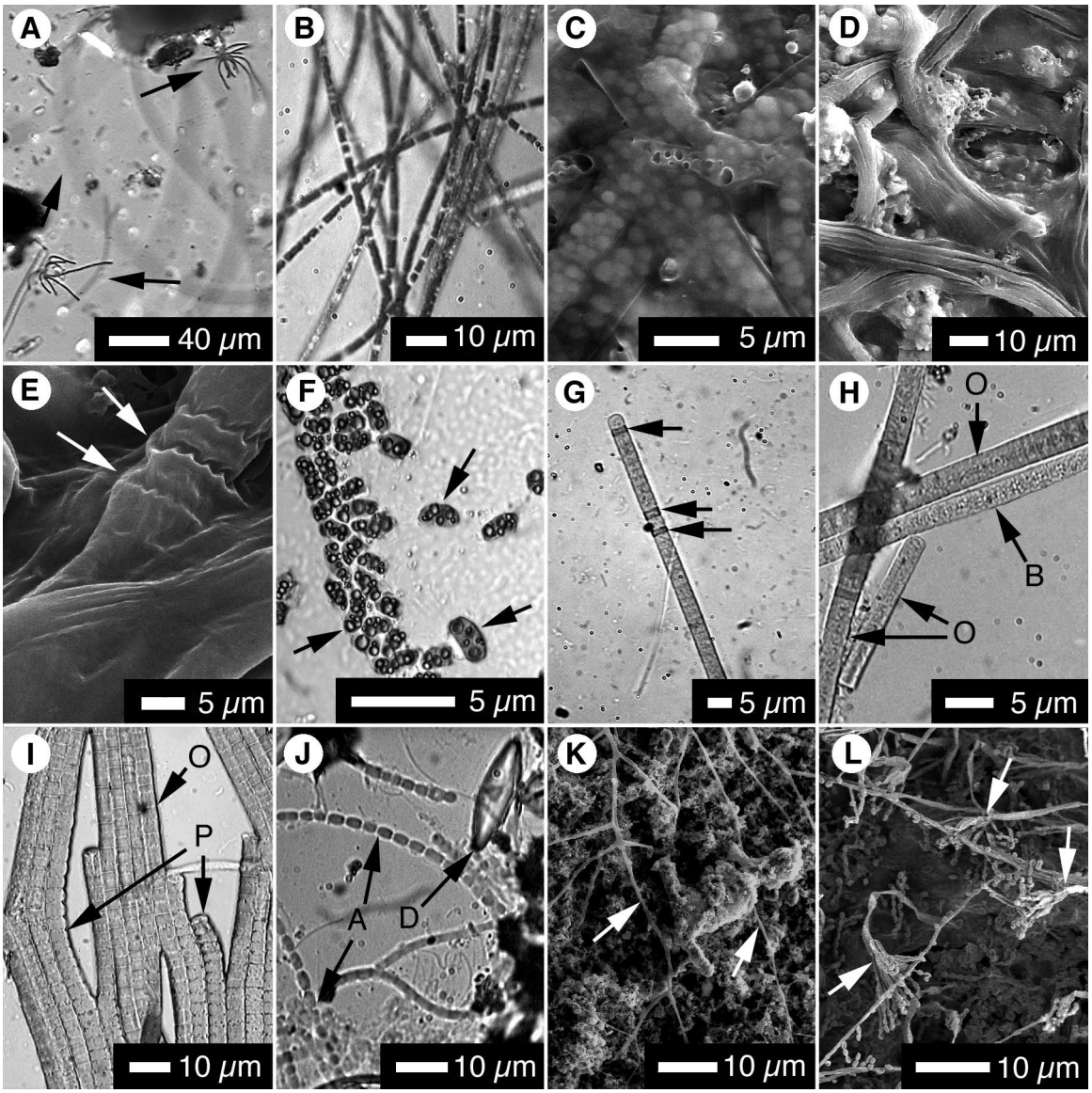

aments have cellular compartments that are locally filled by barite (Fig. 10). Chains of neighbouring cells are in some places baritized together (Figs. 10A, 10B), but it is also common to find filaments of *Beggiatoa* or *Thiothrix* in which only one cell, or several adjacent cells, are barite filled, and surrounding cells appear viable (Figs. 10C–10E). Barite precipitation is limited to the cell cavity, or cytoplasmic chamber, and does not appear to affect septae, nor cell walls (Figs. 10A, 10B). In no instance was a filament found that was both filled and coated or permineralized by barite. Indeed, in many instances barite-filled filaments were found among completely non-mineralized filaments (e.g., Fig. 10A).

It is difficult to assess the crystal morphology of the cell-filling barite because it is surrounded by intact cell walls (Fig. 10E). Detrital, unimodal cylindrical grains composed of nanometric anhedral barite are locally abundant among desiccating *Beggiatoa* streamers, however, and may represent cell-filling barite released from degrading filaments (Fig. 10F).

In the sulphide-rich proximal spring flow path, *Beggiatoa* and *Thiothrix* filaments are commonly packed with 1.5 μm spherical inclusions identifiable as sulphur globules by their refractory appearance in crossed polar light microscopy and EDX analysis. Detrital chains of intergrown, subcrystalline sulphur spheres are released upon cell death (Fig. 11A). Morphologically analogous chains of intergrown subspherical barite were also found among desiccating streamer colonies and are dispersed in *Beggiatoa*-rich mats in stream-fed ponds (Figs. 11B, 11C). In some specimens barite spheres are

Fig. 4. Fresh mineral precipitates from Flybye Springs. (A) Mineral encrustation on glass slide retrieved from below spring D2. (B) Mineral encrustations on rocks and detrital organics proximal to spring D2 (arrows). (C) scanning electron microscopy (SEM) image of sample collected from image B. (D) Detail backscattered electron SEM image of previous sample showing an algal cyst (a), diatoms (d), extracellular polysaccharides (eps) and detrital barite (b). (E) Elemental sulphur rhombs (r) and globules (g) trapped in EPS (eps).

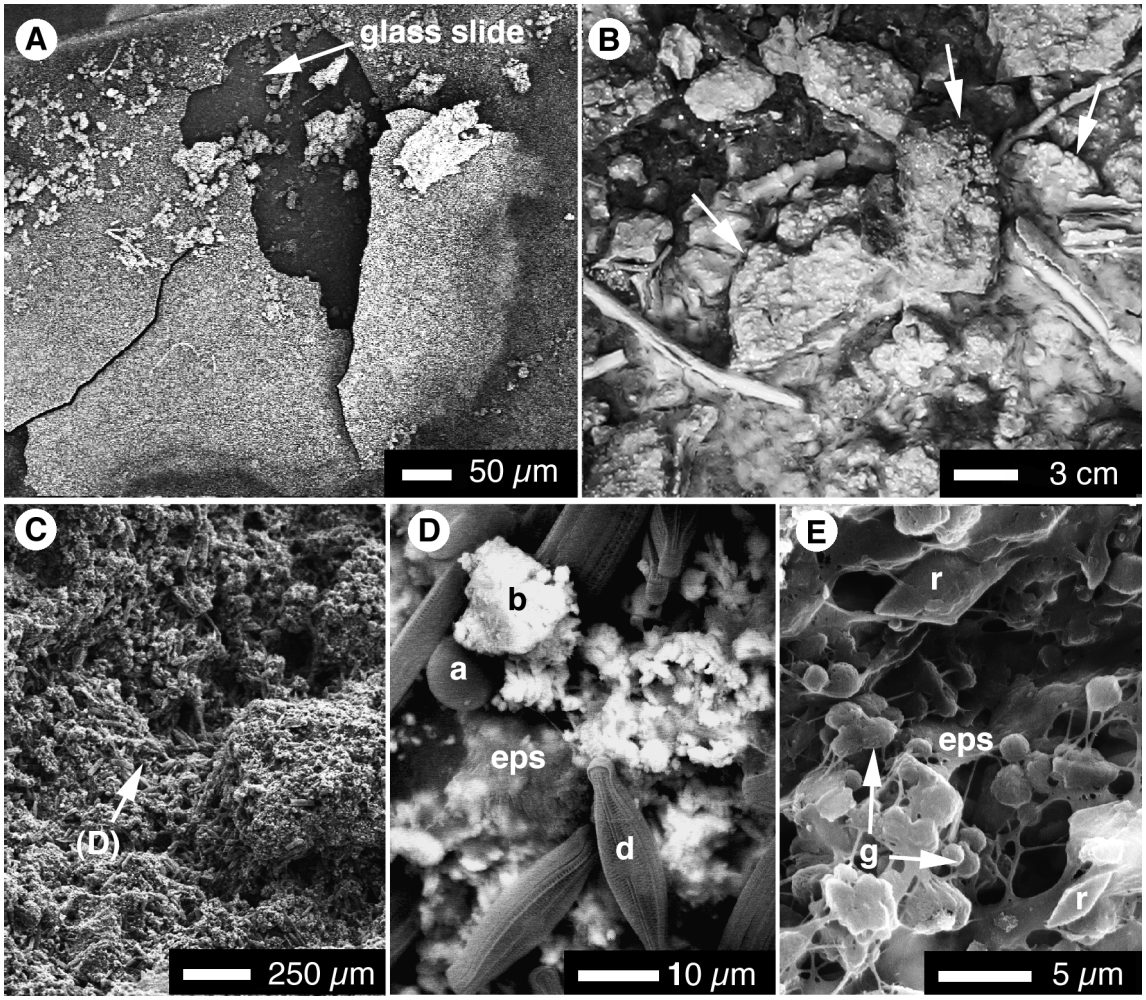

aligned along lysed filaments (Figs. 11D, 11E), indicating that they may have formed intracellularly. A cluster of *Chromatium* found on the slide retrieved from the D2 flow path was found to contain both intracellular sulphur globules and barium-enriched intracellular inclusions (Fig. 11F).

Discussion

Barite crystal habit varies as a function of the degree of saturation (Torres et al. 2003), the chemistry, and the viscosity of precipitating solutions (Sasaki and Minato 1982; Radanovic-Guzvica 1999; Su et al. 2002). The wide array of barite crystal forms found in fresh precipitates reflects the physiochemical and biological diversity of the Flybye Springs flow paths. Barite precipitates through three potential mechanisms at Flybye Springs: (1) inorganically from barite supersaturated solutions; (2) by passive biologic mediation, in the presence of living or dead biomass; and (3) by active biologic mediation, in the presence of fungi and sulphur-metabolizing bacteria.

Proximal to the vents, spring water achieves barite supersaturation via rapid oxidation of H_2S to SO_4, and stellate and tabular barite microcrystals form in solution. Beyond ~5 m of the spring vents and seeps, inorganic barite nucleation is likely inhibited by a combination of lower barium concentrations (due to upstream barite precipitation), decreasing pCO_2 (cf. Lindgren 1933; Bolze et al. 1974), the presence of organic leachates derived from surrounding vegetation (cf. Smith et al. 2004), and sequestration of barium and sulphate in microbial biomass.

The stellate barite crystals found at Flybye Springs are typical of those precipitated at the air–water interface in barite-supersaturated solutions (Sermon et al. 2004); whereas platy barites are more typical of precipitation at interfaces between oxidized and reduced solutions (Stark et al. 2004; Wagner et al. 2005). Scalloped crystals (Fig. 5B) usually form by very rapid precipitation (cf. Stark et al. 2004) and likely formed in more strongly barite-supersaturated Flybye spring water than the euhedral, tabular crystals shown in Fig. 5D (cf. Shikazono 1994; Greinert et al. 2002).

Although composite blocky barite balls form in close contact with microbial cells (Fig. 5F), they are also thought to form inorganically. They are found only among porous de-

Fig. 5. Inorganic barite precipitated from Flybye Springs. (A) Stellate barite microcrystals (arrows) among elemental sulphur globules. (B) Scalloped platy barite microcrystal (arrow). (C) Tabular barite microcrystals surrounded by extracellular polysaccharides (eps) and microbial filament. (D) Close view of tabular barite microcrystals. (E) Composite blocky barite ball (arrows) trapped in EPS (eps). (F) Microbial cells forming casts (arrows) in blocky barite crystal.

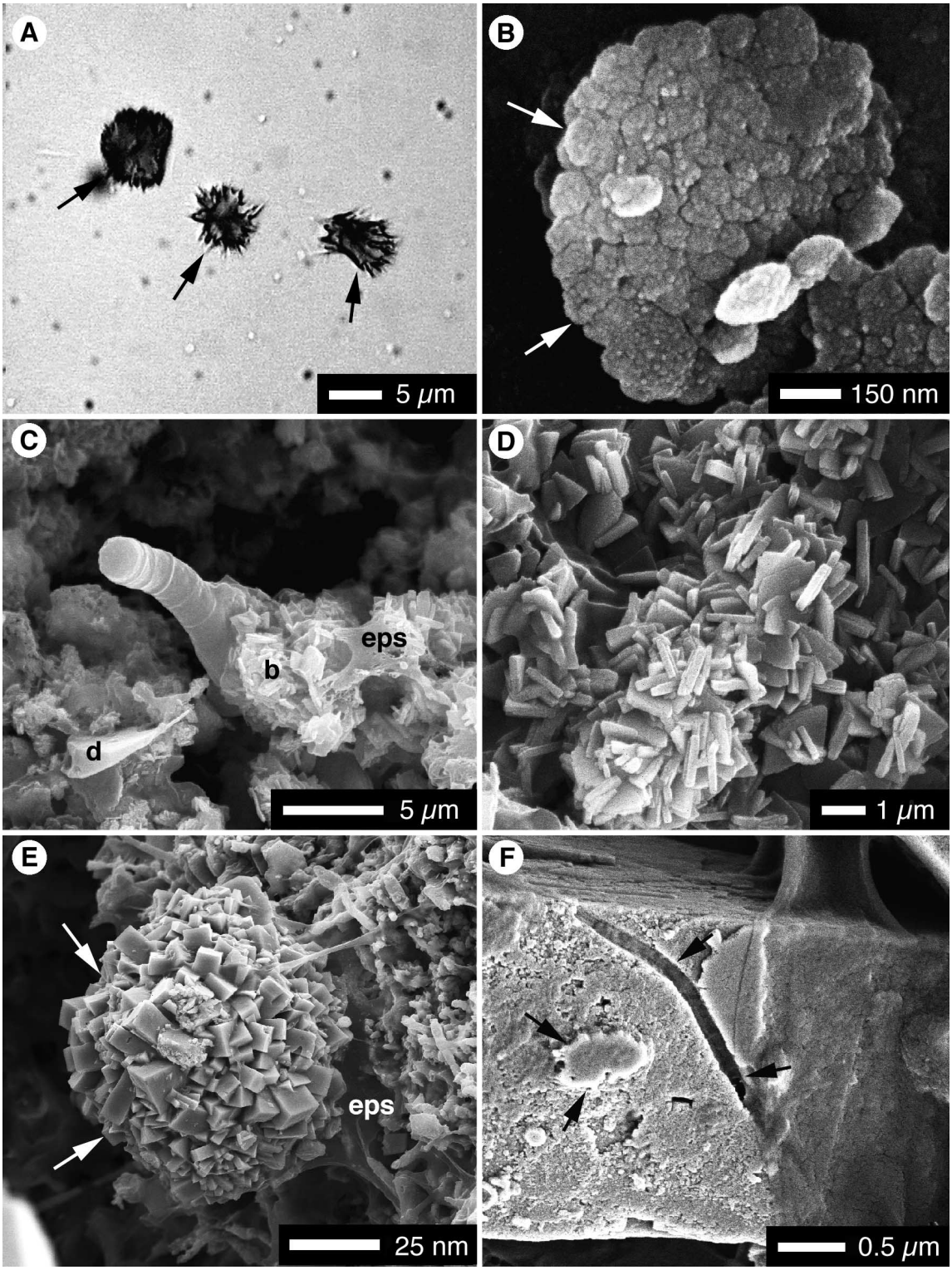

bris (most commonly, clumps of caribou hair) in proximal flow path tributaries at Flybye Springs. Turbulence incited by such obstacles drives rapid oxidation of spring water flowing through them and probably facilitates precipitation of the composite barite balls. Analogous balls of blocky calcite have been described from a hot sulphur spring flow path, where they are associated with high rates of CO_2 degassing (Bonny and Jones 2003).

Fig. 6. Barite laminae in floating microbial mats. (A) Backscattered electron SEM image of barite lamina in stream-fed pond mat. Locations of (C) and (D) shown. (B) Backscattered electron SEM image of barite laminae in vent-fed pond mat (arrows). (C) Upper boundary of barite lamina from (A) (arrows) showing filamentous cyanobacteria and diatom above, granular barite below. (D) Lower boundary of barite lamina from (A) (arrows) showing detrital diatom frustules, decaying organics, and sulphur-metabolizing microbes below and granular barite above. **S** indicates sulphur inclusions. (E) Sparse barite lamina below leaf cuticle from floating "leafy mat"— barite spherules in three sizes, small (**S**), medium (**M**), large (**L**). (F) Detail of medium-sized barite spherule from leafy mat barite lamina. (G) Detail of small barite spherule from leafy mat barite lamina.

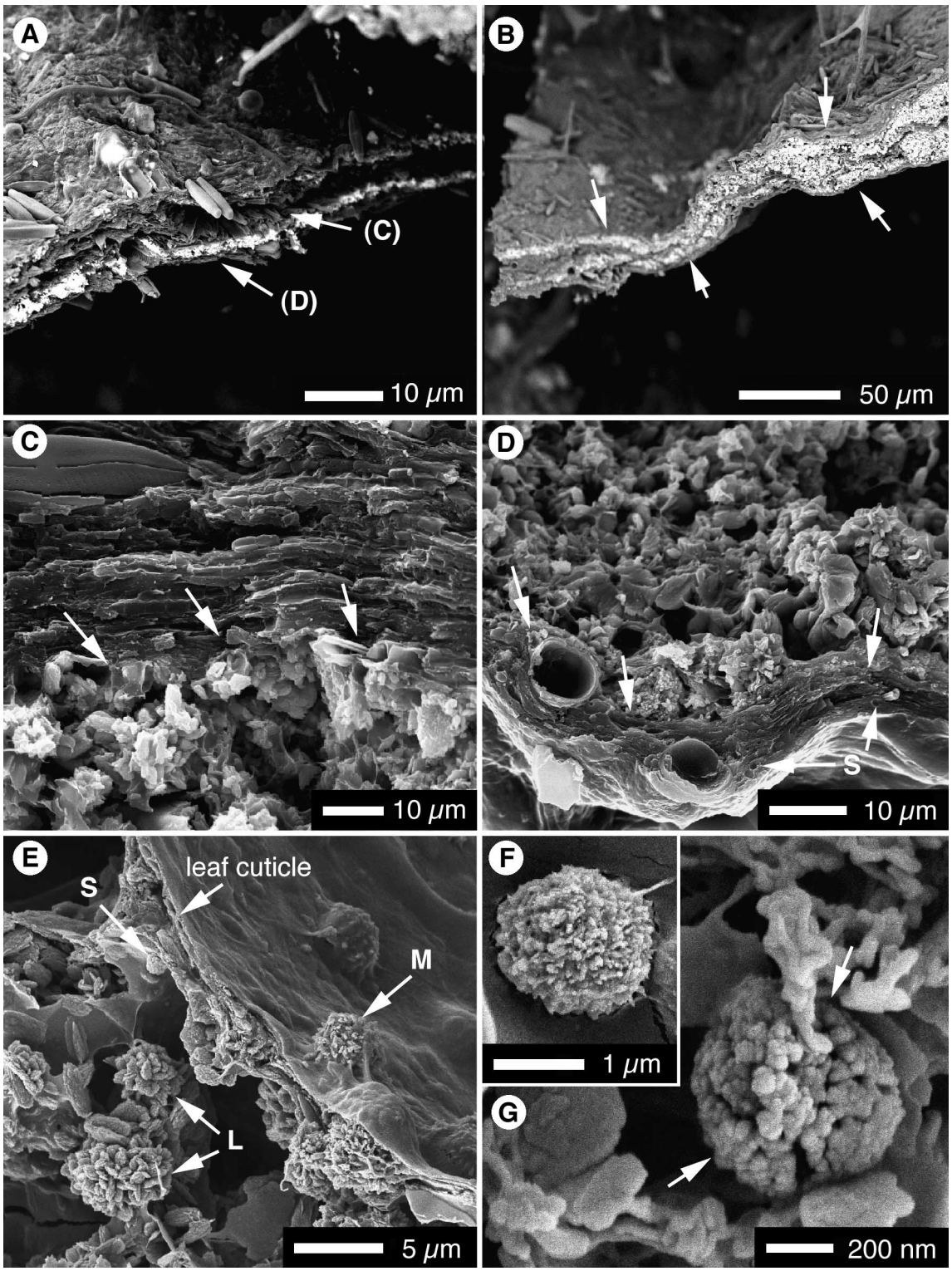

Fig. 7. Barite coating and encrusting microbial cells. (A) Nanometric barite globules (arrows) concentrated near tip of fungal hypha. (B) Barite coated and encrusted *Thioploca* sheath. Locations of (C) and (D) shown. (C) Cross-section of *Thioploca* filament in B. (D) Detail of sparsely mineralized part of *Thioploca* filament showing random arrangement of nanometric barite globule coating. (E) Two single-celled bacteria (arrows) with cell encompassing globular barite coatings. (F) Backscattered electron SEM image of barite encrusted *Thioploca* filaments with casts of sulphate-reducing bacteria (arrows).

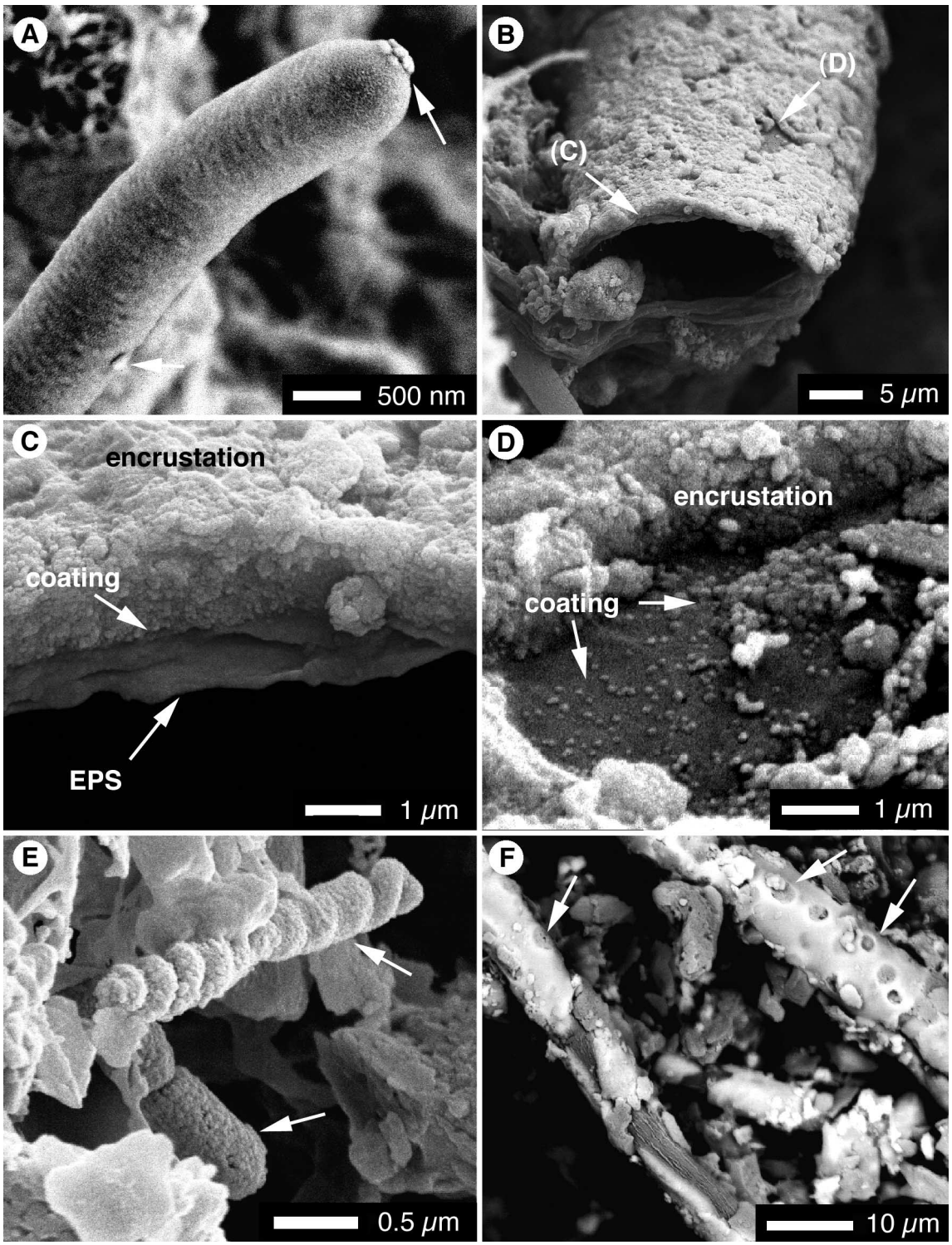

Despite the lack of textural evidence for a microbial influence on "inorganic" barite precipitation, barite solubility in the proximal flow paths may be subtly influenced by bacterial metabolism. Biological sulphur oxidation may contribute to the production of dissolved sulphate for barite precipitation (cf. Senko et al. 2004), and the ~4‰ fractionation between $\delta^{34}S_{sulphide}$ and $\delta^{34}S_{sulphate}$ in the proximal D1 flow path probably arises from bacterial sulphate reduction (cf.

Fig. 8. Barite encrusting microbial cells. (A) *Thioploca* filament with subhedral crystals (2nd layer) on top of anhedral encrustation (1st layer). (B) Heavily encrusted filament. (C) Detail of surface of encrusted filament in B showing intergrown subhedral platy crystals. (D) Detrital tunnel-shaped grain with outer layer of detrital barite trapped in EPS (eps).

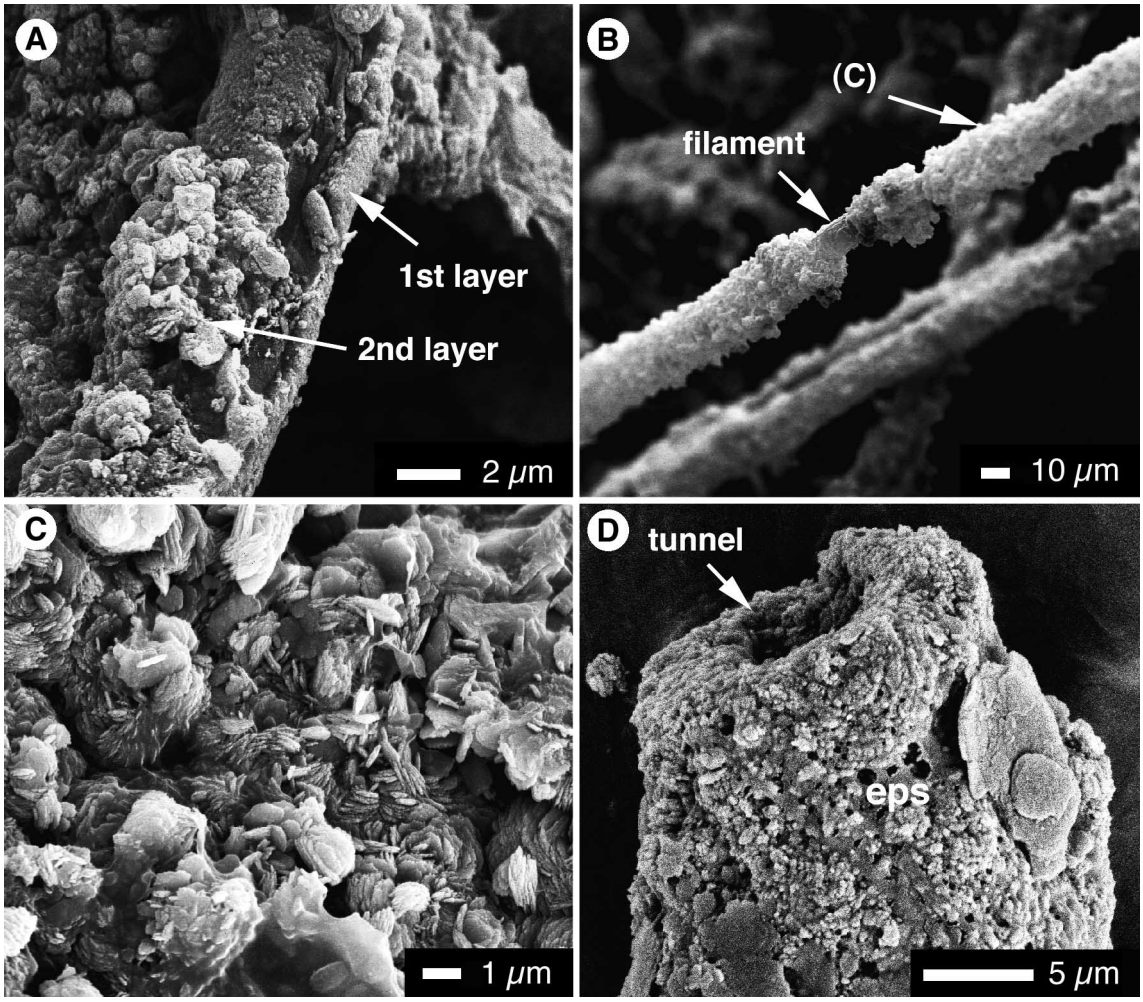

Torres et al. 2003; Canfield 2001). Atmospheric oxidation in the distal flow path produces dissolved sulphate with $\delta^{34}S_{sulphate}$ values much lower than those measured proximal to the vents (14.3‰–15.5‰ vs. 17.3‰–19‰), indicating that sulphate in the distal flow path is derived by oxidation of bacterially reduced sulphur. Sulphate reducing bacteria counteract atmospheric oxidation of the spring water, prolonging dysoxic conditions in the Flybye Springs flow paths and thus limit inorganic barite precipitation window to the proximal flow paths. Prolonged dysoxia also extends the environmental niche favoured by redox boundary sulphur-oxidizing bacteria.

Biologically mediated barite precipitation takes place throughout the Flybye Springs flow paths but is most important outside the inorganic barite precipitation window. Microbial mats and biofilms are generally enriched in divalent cations due to the adsorptive capacity of microbial cells and EPS (Arp et al. 1999; Schultze-Lam and Beveridge 1994). Barium enrichment in microbial mats and biofilms growing in barium-rich solutions is well documented (e.g., Douglas and Douglas 2001; Tazaki and Watanabe 2004), and secondary exposure to dissolved sulphate may induce precipitation of subhedral barite microcrystals in microbial biomass (Tazaki et al. 1997; Sanchez-Moral et al. 2004; Glamoclija et al. 2004). Direct nucleation of barite on microbial surfaces has not been documented from a natural setting, however, nor have microbial mats with discretely baritized laminae.

The development of barite laminae at Flybye Springs is attributable to redox stratification in floating mats, which prevents homogeneous exposure to dissolved sulphate. In vent-fed ponds, barite laminae form between *Beggiatoa* and *Oscillatoria* layers—a transition that usually spans an oxic–anoxic boundary (Larkin and Strohl 1983; Jørgensen and Des Marais 1986). Barite precipitation may also be limited in the lower levels of floating mats by SRB-established anoxia among degrading filaments. The thickness of the baritized laminae probably corresponds to the thickness of the redox boundaries in the floating microbial mats, with barite undersaturated on the lower side because of a lack of sulphate, and supersaturated in barium-enriched EPS above.

The top layers of floating mats may escape baritization because of a directional barium source. Evaporative wicking at the mat surface (cf. Arp et al. 1999), and directional barium delivery from a vent source below the mats, would favour upward diffusion of barium. Fixation of this barium by

Fig. 9. Barite permineralized microbial cell walls (arrows). (A) Side view of permineralized filament with diameter corresponding to *Beggiatoa* or *Oscillatoria*. (B) Cross-section of permineralized filament. (C) Detail of surface of permineralized cell with diameter corresponding to *Thiothrix*. (D) End of filament showing encrusting barite (e), permineralized cell wall (p), and infilling precipitates (f). Location of (E) is shown. (E) Detail of filament in (D) showing distinction between permineralizing barite globules (p) and encrusting platy crystals (e). (F) Three-layered detrital grain.

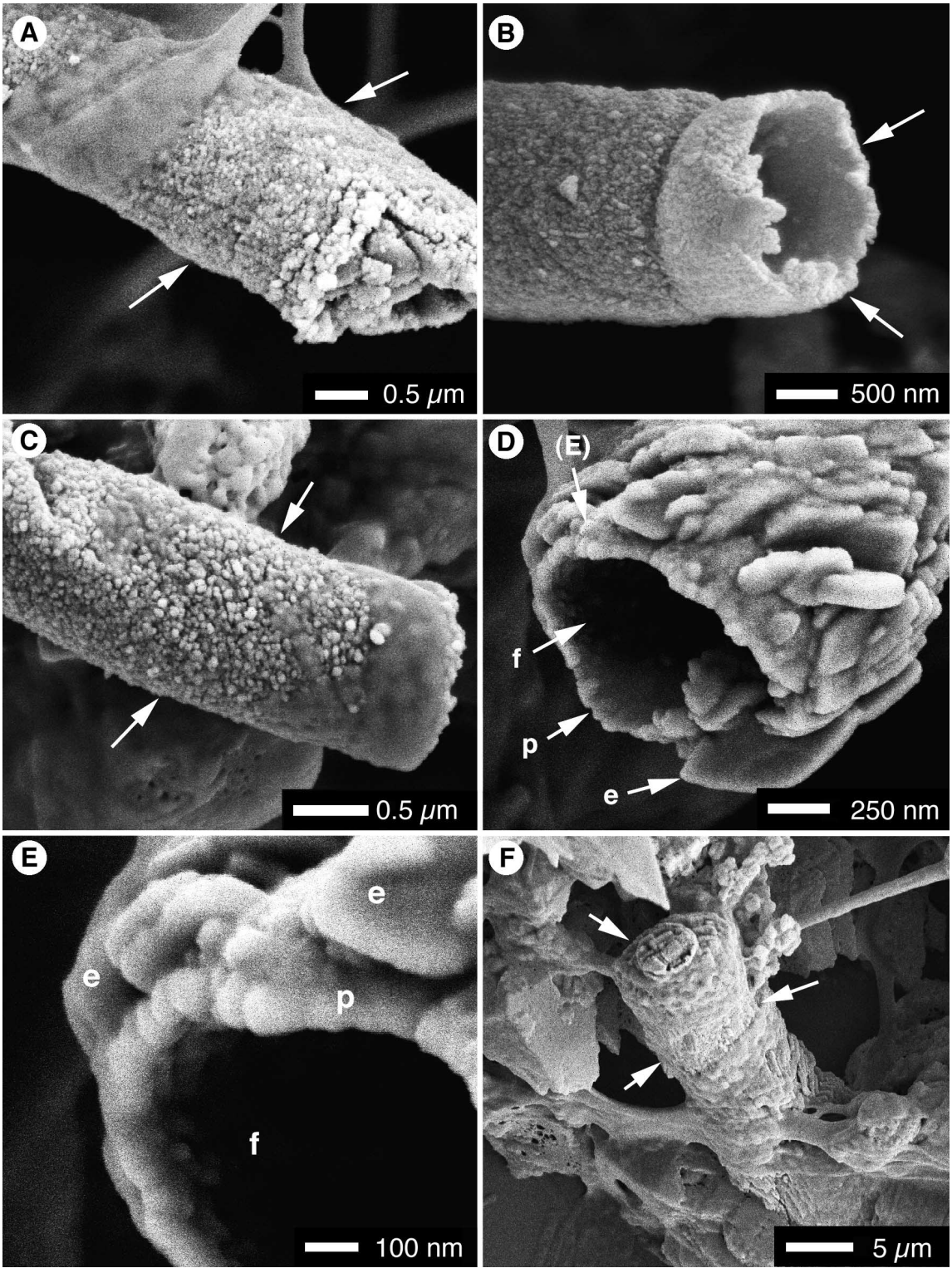

precipitation at the redox boundary (cf. Torres et al. 2003) might prevent mineralization of the upper mat layers, allowing upwards microbial growth. The subhedral and anhedral granular barite microcrystals found in the barite laminae are similar to laboratory barite precipitated from highly supersaturated solutions (cf. Bala et al. 2005), which supports the

Fig. 10. Barite filled microbial cells. (A) Barite filled *Beggiatoa* filament (arrows) among non-mineralized filaments. (B) Backscattered electron SEM image of barite filled cells in *Beggiatoa* and *Thioploca* filaments; note that cell walls and septae are not mineralized (arrows). (C) Crossed polar light microscope image of *Thiothrix* filaments with isolated groups of barite filled cells (arrows). (D) Two barite filled cells in *Thiothrix* filament (arrows). (E) Chain of barite filled cells embedded in EPS (arrows indicate septal breaks). (F) Unimodal microcrystalline detrital grains which may represent barite released from degrading filaments (arrows).

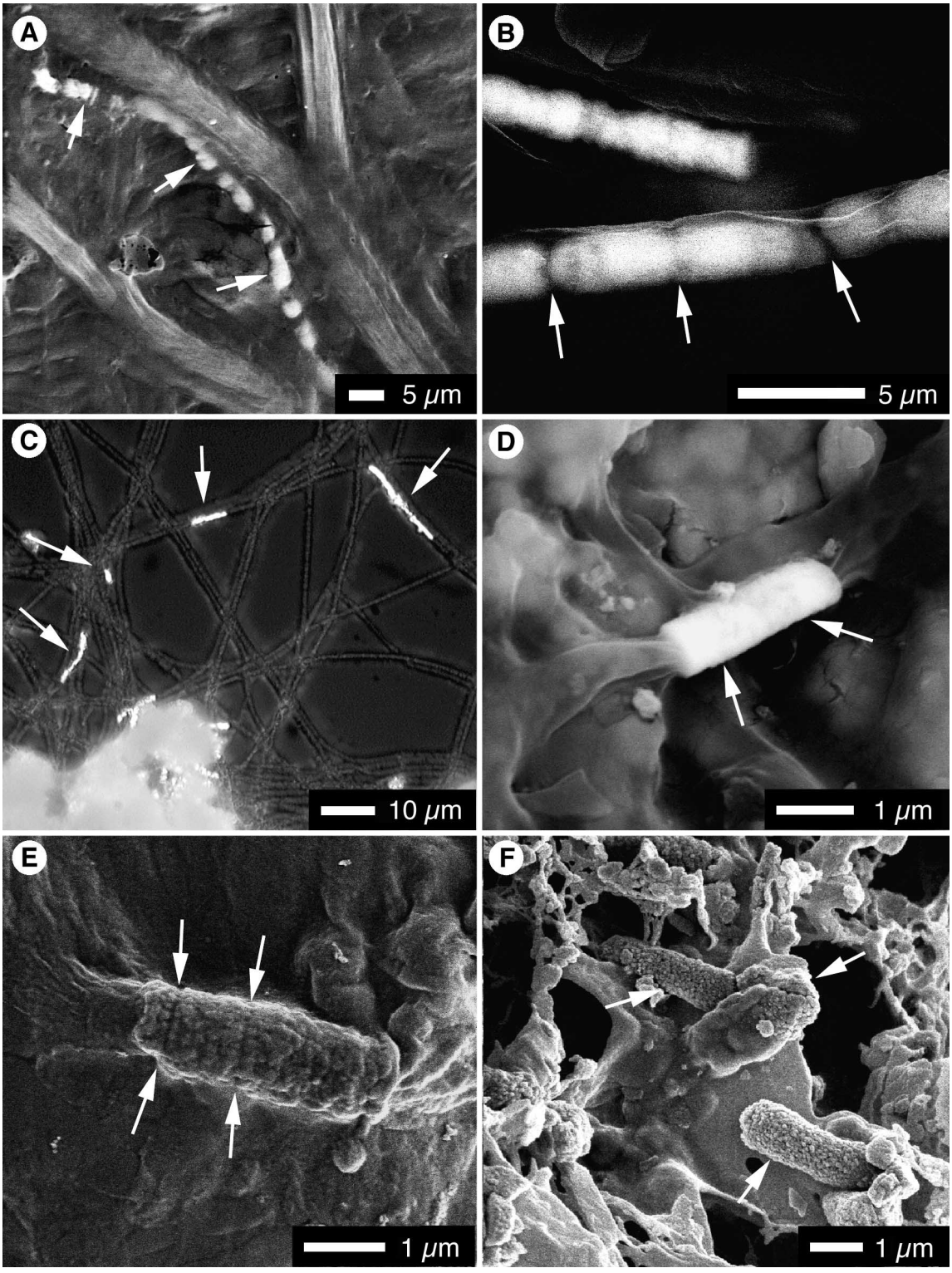

idea that the redox boundary is an efficient barium immobilizer. As mat growth proceeds upwards, vertical migration of the redox boundary might generate the stacked barite laminae found in some mats.

Fig. 11. Bacteriogenic sulphur and barite globules. (A) Detrital elemental sulphur chains (arrows). (B, C) Detrital barite spheres in secondary electron and backscattered electron SEM images (arrows). (D, E) Detrital barite spheres aligned along a lysed filament in secondary electron and backscattered electron SEM images (arrows). (F) Backscattered electron SEM image of Chromatium cells with elemental sulphur (S) and barium-enriched inclusions (Ba).

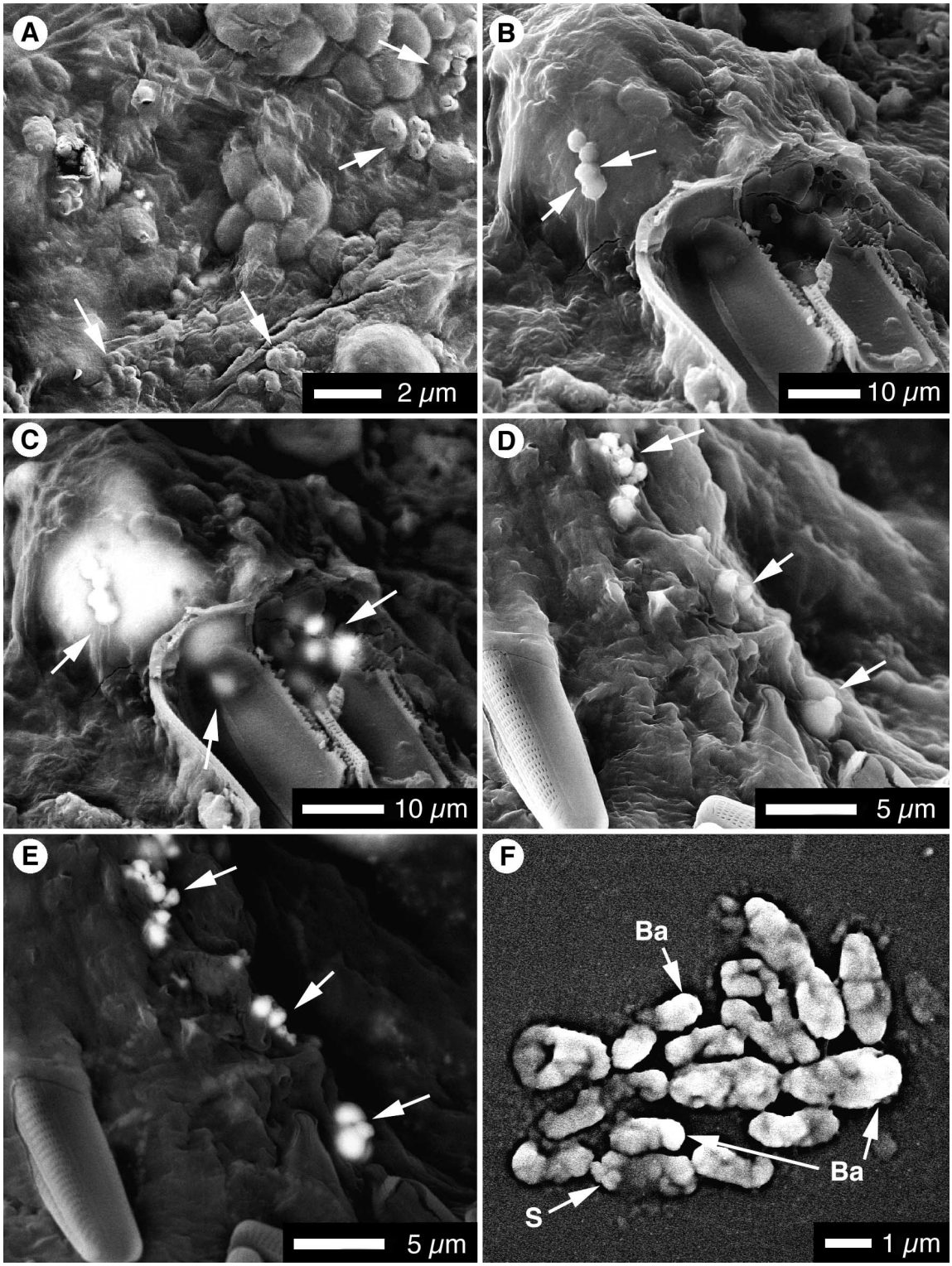

The arrangement of barite spherulites in "leafy mats" may likewise be determined by a local redox boundary between anoxia in degrading leaf tissue and oxygenated fluids across the outer, waxy cuticle. The leaf-associated spherulites are similar in size and morphology to barite spherulites experimentally precipitated in solutions rich in fulvic acid by Smith et al. (2004). Humic acids, including fulvic acid, inhibit barite nucleation and crystal growth (Smith et al. 2004)

and may be responsible for the morphological distinction between the leaf-associated and other mat-bound barite laminae at Flybye Springs. Ultimately, the barite laminae formed as a result of barium enrichment in microbial biomass. In this regard, the laminae may be considered biologically mediated (cf. Braithewaite and Whitton 1987), but degrading leaves are equally able to induce barite precipitation as microbes. True microbial biomineralization at the Flybye Springs occurs in direct contact with microbial cells.

Microbial surfaces are generally negatively charged due to the presence of carboxyl and phosphoryl groups in the outer cell membrane (gram-negative bacteria), peptidoglycan layer (gram-positive bacteria), or EPS sheaths (Schultze-Lam and Beveridge 1994; Fortin et al. 1998). Binding of cations to these sites promotes the binding of counterions and can thus facilitate mineral precipitation. In this scenario, biomineralization takes place passively, as a result of the chemical properties of the external cell surface (cf. Leadbeater and Riding 1986). Passive biomineralization has been invoked to explain the formation of microbial molds or tubes in silica (Konhauser et al. 2003), calcite (Merz-Preiß 2000), zinc and arsenic sulphides (Douglas and Douglas 2001; Jackson et al. 2001), and iron oxides (Fortin et al. 1998), but has never before been reported in barite.

At Flybye Springs, primary barite coatings and secondary encrustations are common on and around various microbial genera. Concentration of barium on cell and sheath surfaces would lower the activation energy for barite in close proximity to microbial cells exposed to sulphate. In dysoxic Flybye spring water, sulphate sourced from atmospheric and microbial sulphur oxidation could react with adsorbed barium to precipitate barite globules on microbial cells. Barium adsorbed to the EPS sheaths of *Thioploca* would have less opportunity to interact with dissolved sulphate because of the anoxia that prevails in the methane-rich, vent-fed bottom waters of the ponds that *Thioploca* inhabits. Hydrated methane has been reported to decrease barite solubility, however, so vent-sourced methane may actually promote barite precipitation on *Thioploca* sheaths exposed to even trace amounts of sulphate (cf. Tomson et al. 2003).

Localization of barite globules around hyphal tips suggests that distinct processes control barite solubility around fungi. Fungi have a subcrystalline protein latticework, called chitin, imbedded among polysaccharides in their outer cell wall. Chitin contains a variety of anionic subgroups, including phosphate, carboxyl, and sulphydryl groups, but does not readily bind divalent cations and resists mineralization (Gadd 1993). Mineral precipitation on fungal hyphae thus takes place either around degrading cells or as a by-product of energy-dependent cellular processes related to detoxification (Gadd 1993).

Fungi growing in barium-rich solutions employ several mechanisms to avoid barium toxicity, including sequestering barium ions into inert precipitates, preventing barium uptake by secreting chelating enzymes, and actively flushing barium ions from the cell after accumulating them in cytoplasmic vacuoles (Aruguete et al. 1998; Mukherjee et al. 2001; Weber 2002; Steiman et al. 2004). Both secretion of chelating enzymes and flushing of metal-enriched vacuoles take place at the apex of fungal hyphae (Gadd 1993; Weber 2002) and could produce a barium-enriched microenvironment around hyphal tips that would favour barite precipitation in sulphate-bearing solutions.

Fungi growing in sulphide-rich solutions also battle sulphide toxicity, and many detoxify by carrying out nonmetabolic sulphur oxidation (Natorff et al. 2003). In this process, sulphur is oxidized intracellularly, and sulphate ions are complexed with the enzyme sinigrin, which is expelled to release sulphate extracellularly (Sakorn et al. 2002). When hyphae are grown on barium-enriched agar, this process induces rapid precipitation of barite around sulphur-oxidizing cells (Sakorn et al. 2002). Reaction of barium dissolved in spring water with fungally sourced sulphate could also drive precipitation of barite globules around fungal tips in the Flybye Springs flow path.

Irrespective of the detoxification process involved, *Penicillium* can be considered to be actively biomineralizing at the Flybye Springs, precipitating barite as a by-product of physiological processes (cf. Leadbeater and Riding 1986). Precipitates nucleated against microbial substrates are generally small, hydrated, and amorphous (Douglas and Douglas 2001), but can act as substrates for the growth of secondary crystalline phases. Gonzalez-Munoz et al. (2003) induced barite precipitation around bacteria (*Myxococcus xanthus*) growing in barium-enriched agar, and observed a progression from spherical to rhombic barite precipitation, similar to the crystallographic change from globular coatings to crystalline barite encrustations. It can be suggested that once the nucleation threshold is crossed by formation of barite globules on microbial surfaces at Flybye Springs, barium and sulphate are able to diffuse towards the globule surface from the spring water, allowing growth of secondary barite encrustations.

Barite permineralization of cell walls requires that barium and sulphate ions diffuse through the outer cell surface. Permineralization was observed only in filaments of *Thiothrix*, *Beggiatoa*, and *Oscillatoria*. These are all redox interface organisms (Jørgensen and Des Marais 1986; Nelson 1987; Garcia-Pichel and Castenholz 1990) found near oxic–anoxic interfaces, where sulphate is not expected to limit barite saturation; once again, barite precipitation requires concentration of barium, this time within the outer cell layer. The fact that members of these genera are permineralized, rather than simply coated, may arise from the distinct properties of their outer cellular surfaces.

Neither *Oscillatoria* nor *Beggiatoa* form EPS sheaths, and sheath formation in *Thiothrix* is inconsistent and probably environmentally determined (Reichenback 1981). No sheathed *Thiothrix* filaments were found in samples from Flybye Springs.

This lack of an EPS sheath may be important to facilitating permineralization as it allows barium ions to diffuse unimpeded towards the external cell surface (cf. Oehler and Schopf 1971). Binding of barium in EPS may, in fact, prevent permineralization of *Thioploca* sheathed filaments, despite their morphological similarity to *Beggiatoa* and *Oscillatoria*.

Beggiatoa, *Thioploca*, and *Oscillatoria* have similar multilayered cell walls, in which only the inner layers (cytoplasmic membrane and murein layers) participate in septation, and outer layers are continuous along the length of the filaments (Larkin and Strohl 1983; Teske and Nelson 2005).

The outer layers of all three genera include an outer membrane, a peptidoglycan wall, a gram-negative cell envelope, and, in some species, subcrystalline fibrillar arrays of proteins, which may facilitate cation adsorption to the outer cell surface (Larkin and Strohl 1983; Adams et al. 1999). *Beggiatoa* and *Oscillatoria* also have similar perforations through their peptidoglycan walls, which are arranged near septal cross-walls in both microbial groups (Palinska and Krumbein 2000). The cellular structure of *Thiothrix* is not as well documented but is generally considered to be simpler, composed of an inner cytoplasmic membrane, a peptidoglycan cell wall, and an outer cellular envelope (Larkin and Strohl 1983; Teske and Nelson 2005).

Silica permineralized microfossils are common in the geologic record and are thought to form by nucleation of silicic acid on reactive carboxyl, hydroxyl, and phosphoryl groups within the permineralizing "organic template" (Westall 1999; Konhauser et al. 2003). Subsequent polymerization of silica then preserves the organic structure. A similar mechanism is proposed here for permineralization by barite wherein barium cations are adsorbed to reactive groups in the organic template and subsequently complex with dissolved sulphate to form barite globules that preserve the organic structure. In thick-walled filaments of *Beggiatoa* and *Oscillatoria*, the peptidoglycan layer perforations may be important to the permineralization process. These structures are thought to function as transport pathways between the cytoplasm and external solutions (Palinska and Krumbein 2000) and may facilitate barium diffusion into thick, multilayered cell walls at Flybye Springs.

Barite precipitation inside cellular cavities requires transport of barium through cell walls. Intracellular barite precipitation at Flybye Springs takes place in *Beggiatoa* and *Thiothrix* filaments that are commonly surrounded by completely nonmineralized cells of the same and other genera. Clearly, intracellular barite precipitation takes place where barite supersaturation is achieved inside, rather than around, microbial cells.

Barium enrichment in cytoplasmic fluids has been reported for various microbial groups, including fungi (Cormack et al. 1975; Grupe and Herrmann 1988), green algae (Mann and Fyfe 1984; Ganeshram et al. 2003), and diatoms (Vinogradova and Koval'skiy 1962). Above a certain concentration, however, barium bioaccumulators approach a toxicity threshold (Baldi et al. 1996) and must actively rid themselves of barium, sequester barium in an inert form, block further transport of barium into their cells, or die (Aruguete et al. 1998).

In the Flybye spring waters microbes are exposed to barium concentrations up to 12 ppm (this paper, Table 1), which are well above seawater and continental freshwater norms of 5 and 54 ppb (Bolze et al. 1974). Barium toxicity may be a plausible explanation for intracellular barite precipitation in *Beggiatoa* and *Thiothrix* at the Flybye Springs, as a cellular mechanism to combat metal toxicity has not been documented for either genera.

If cytoplasmic barium concentrations achieved toxic levels and induced the death of single cells, or groups of cells along a filament, they would cease osmoregulation and dissolved sulphate might be able to diffuse across the cellular membranes, producing barite supersaturated conditions inside the cell. If there were ambient sulphate and high barium concentrations in fluids surrounding the microbes, however, it is a mystery as to why their cell walls were not permineralized, coated, or encrusted. One explanation might be that the sulphate was sourced within the boundary of the cell wall—perhaps from oxidizing sulphur globules. An intracellular sulphate source would also explain why *Oscillatoria*, which is morphologically similar to *Thiothrix* and *Beggiatoa* but does not accumulate intracellular sulphur granules, does not experience intracellular barite precipitation at Flybye Springs.

Filaments of *Beggiatoa*, *Thiothrix*, and *Chromatium* throughout the Flybye spring flow paths and ponds contain numerous intracellular sulphur globules. The composition of bacteriogenic sulphur globules varies between microbial genera, and within single genera, growing in distinct physiochemical environments. Pasteris et al. (2001) found inclusions in marine *Beggiatoa* strains that are composed of relatively pure fine-grained, microcrystalline sulphur in a protein envelope; but in most cases, sulphur inclusions have lower density than crystalline elemental sulphur (Mas and van Gemerden 1987). In filamentous sulphur-oxidizing bacteria, sulphur globules are commonly composed of metastable fluid polythionates (Steudel 1989; Pattaragulwanit et al. 1998), whereas sulphur globules in anoxygenic phototrophs are dominated by sulphur chains (Prange et al. 2002).

Oxidation of any composition of sulphur globules to sulphate in a barium-enriched cytoplasmic chamber could initiate rapid precipitation of barite in the cellular cavity. Oxidation of intracellular sulphur globules has been reported to occur spontaneously upon cell death (Brigmon et al. 1994). It is more common, however, for sulphur globules to crystallize as elemental sulphur (Steudel 1987). Cells with densely packed sulphur inclusions may, in fact, be "permineralized" by elemental sulphur crystals that breach globule-restraining membranes soon after cell death (Ohno and Tazaki 2000). Oxidation of permineralizing sulphur in a barium-enriched cytoplasmic chamber exposed to oxygen-rich fluids by degradation of the cell wall could provide a means to baritize the intracellular cavity wholesale, as is found in many of the *Beggiatoa* and *Thiothrix* filaments at Flybye Springs (Fig. 10).

Apparent baritization of sulphur globules (Fig. 11) is more difficult to explain. Sulphur globules in *Thiothrix* and *Beggiatoa* are located inside the outer cell wall, but are restricted to invaginations of the cytoplasmic membrane and further surrounded by a "sulphur-inclusion envelope"; they do not come into contact with cytoplasmic fluids (Larkin and Strohl 1983; Nelson 1987; Larkin and Henk 1996). Sulphur globules in *Chromatium* are dispersed in the cytoplasm but surrounded by extracytoplasmic vesicular membranes that prevent contact between the contents of the sulphur globule and the cytoplasm (Pattaragulwanit et al. 1998; Reinartz et al. 1998). Precipitation of barite within the globule-restraining membrane thus necessitates barium diffusion from the cytoplasm into the sulphur globule. This might take place if the cell were approaching a barium toxicity threshold and lost its ability to regulate transport of ions across the cytoplasmic membrane. Alternately, the sulphur globules themselves may have become barium enriched.

Some sulphur globules have been found to incorporate organic molecules (Mas and van Gemerden 1987) and up to 5% iron, calcium, silica, aluminum, and magnesium (Douglas and Douglas 2000). Anionic groups in the sulphur globules or their restraining membranes render them hydrophilic (Steudel 1989), and trace element enrichments may be explained by adsorption of cations to these charged sites. Barium could potentially be adsorbed likewise, and oxidation of barium-enriched sulphur globules might initiate barite precipitation in the sulphur globule restraining membrane without supplying sulphate to the cytoplasm. This process could take place upon cell death and desiccation, but the barium-enriched inclusions found in *Chromatium* (Fig. 11F) suggest that sulphur globules can become barium enriched (or baritized) in viable cells.

Metabolic oxidation of sulphur globules to sulphate is carried out by *Chromatium*, as well as select species of freshwater *Thiothrix* and *Beggiatoa* (Nelson 1989; Patritskaya et al. 2001). Complete oxidation of sulphate generally only takes place, however, in stressed environmental conditions; for example, in light-restricted *Chromatium* colonies (Overmann and Pfennig 1992) or among bundles of sulphur-oxidizing bacteria stranded in low-sulphide waters (Nelson 1989). In *Chromatium*, sulphur oxidation sites are located inside the extracytoplasmic membranes that surround sulphur globules and could produce sulphate for barite precipitation in situ (Pattaragulwanit et al. 1998). Sulphur oxidation in *Beggiatoa* and *Thiothrix* is also thought to be mediated by membrane bound-enzymes, though the process is not well understood (Reinartz et al. 1998; Patritskaya et al. 2001). It is interesting to speculate that, in addition to low sulphide concentrations in desiccating tributaries and in aerated splash zones, stresses associated with barium toxicity might prompt microbes to oxidize their sulphur globules—with unexpected results.

Both cellular cavity-filling barite precipitation and baritization of sulphur globules are ultimately thought to arise as a result of intracellular sulphur storage and (or) barium bioaccumulation and can thus be considered end-products of active biomineralization (cf. Leadbeater and Riding 1986).

Though both passive and active biomineralization have been reported from diverse mineralogies (Knoll 1985; Westall 1999; Riding and Awramik 2000; Jackson et al. 2001), microfossil-generating biomineralization in barite has not been documented prior to this study. Passive barite biomineralization at the Flybye Springs is dependent upon microbial barium concentration via adsorption to cell surfaces and exudates. Active biomineralization proceeds by physiological mediation of barite saturation gradients around and inside microbial cells. Microbial taphonomy in carbonate, silica, and iron oxides has been found to be texturally sensitive to differences in cellular structure, metabolism, and ambient chemistry (e.g., Walter and Des Marais 1993; Arp et al. 1999), which has important implications for their interpretative potential in the geologic record. Generally, microfossils have more textural variability in minerals that can precipitate by both active and passive biomineralization (e.g., calcium carbonate precipitated actively via photosynthetic CO_2 withdrawal or passively by calcium adsorption to cell surfaces and exudates); thus, they provide the most insight into the physiochemical conditions of their environment of formation (Arp et al. 2001; Kaufman and Xiao 2003; Shen et al. 2001).

Active and passive biomineralization processes are associated with distinct microbial genera at the Flybye Springs (with some overlap) and generate texturally specific detrital barite microfossils. Barite laminae, tunnels, multi-layered cylinders, intracellular casts, and sulphur-globule-mimicking grains all bear textural details that are determined in part by the ecology, morphology, cellular structure, and metabolism of the microbes involved in their formation. Such microfossils would have high interpretative potential if preserved in the geologic record.

Barite is highly insoluble and stable through diagenesis if it is sequestered from anoxic solutions (Jewell 2000; Karnachuk et al. 2002) and commonly forms in microbially colonized environments (Carroue 1996; Burhan et al. 2002; Torres et al. 2003; Lu et al. 2004). Indeed, some of the Earth's earliest putative stromatolites formed in barite precipitating environments (Buick et al. 1981; Shen et al. 2001; Kiyokawa et al. 2006). The biomineralization processes taking place at the Flybye Springs offer a rare glimpse into how some of Earth's earliest organisms may have interacted with their geochemical environment and the kinds of microfossil evidence they might have left behind.

Microfossil-generating biomineralization at Flybye Springs takes place where spontaneous inorganic barite precipitation is no longer favoured by spring water physiochemistry. Practically speaking, these microfossils represent fixation of barium from spring water that is ultimately destined for dispersal in the watershed surrounding Flybye Springs. Barium is highly toxic to many plants and animals and creates environmental problems when it leaches into groundwater (Baldi et al. 1996). Barium bioaccumulating fungi have been applied in bioremediation of barium-rich petroleum waste products (Dominguez-Rosado et al. 2004), and barite biomineralizing bacteria might be equally suited to bioremediation technologies. Radioactive barite scale and sludge generated by the hydrocarbon industry are relatively inert under oxic conditions but can be remobilized if they are exposed to anoxic solutions or sulphate reducing bacteria after disposal (Desideri et al. 2006). Dysoxic niche-occupying barite biomineralizing microbes, like those found at Flybye Springs, may be well suited to controlling barium leachates generated at redox boundaries.

Conclusions

The Flybye spring water emerges rich in sulphide and barium, precipitates elemental sulphur and barite, and supports a rich community of sulphur-tolerant and sulphur-metabolizing microbes. Proximal to the spring vents, barite microcrystals precipitate inorganically from barite supersaturated spring water. In distal tributaries and vent- and stream-fed ponds, barite precipitates in direct association with microbes.

Adsorption of barium to negatively charged molecules in microbial cell walls, sheaths, and EPS is considered important to establishing localized barite supersaturation and produces the following passively biomediated and biomineralized precipitates:

(1) Microcrystalline barite laminae at microbially mediated oxic–anoxic boundaries in floating microbial mats.
(2) Nanometric coatings and micrometric encrustations of barite on diverse microbial cells, which generate tunnel-shaped microfossils.
(3) Barite permineralized outer cell layers in *Beggiatoa*, *Thiothrix*, and *Oscillatoria*, which can be encrusted and filled by secondary precipitates to form three-layered microfossils.

Intracellular barium-enrichment and (or) physiologic sulphur oxidation may be important to the formation of actively biomineralized precipitates, including the following:
(1) Nanometric barite globules near the tips of fungal hyphae.
(2) Barite impregnated cellular cavities in non-permineralized *Beggiatoa* and *Thiothrix* filaments.
(3) Baritized sulphur globules produced in and released from *Chromatium*, *Beggiatoa*, and *Thiothrix*.

The variability in biomineralization at Flybye Springs stems from differences in the chemical microenvironment where barite precipitation takes place and differences in cellular structure and metabolic strategy among microbial genera.

Acknowledgements

This project was funded by the Canadian Circumpolar Institute, the Alberta Ingenuity Fund (studentship 200300215 to Sandy Bonny), and the National Science and Engineering Research Council of Canada (grant A6090 to Brian Jones, and Ph.D. Canada Graduate Scholarship to Sandy Bonny). Fieldwork was conducted with the permission of the Aurora Research Institute (License #13590N). Figure 1A is adapted from an image provided by the Aurora Research Institute, Aurora College, Inuvik, N.W.T., Canada.

Thanks are extended to Dr. John Duke at the University of Alberta SLOWPOKE Laboratory; Dr. Karlis Muehlenbachs who consulted on gas collection techniques and analysis; George Braybrook who provided invaluable assistance on the SEM; Dr. Alex Wolfe and Dr. Randy Currah who assisted with microbial identification; and Dustin Rainey who helped in the field. The comments of Dr. Dirk Bosbach and an anonymous reviewer on an earlier draft of this manuscript are much appreciated.

References

Adams, D.G., Ashworth, D., and Nelmes, B. 1999. Fibrillar array in the cell wall of a gliding filamentous cyanobacterium. Journal of Bacteriology, **181**: 884–892.

Al-Jundi, J. 2001. Comparison of neutron activation analysis and inductively coupled plasma – atomic emission spectroscopy for the determination of elements in environmental samples. Dirasat – University of Jordan, Engineering Sciences, **28**: 49–55.

Allen, C.C., Grasby, S.E, Longazo, T.G., Lisle, J.T., and Beauchamp, B. 2002. Life beneath the ice – Earth (!), Mars (?), Europa (?). 33rd Lunar and Planetary Science Abstracts, March 11–15, 2002, Houston, Texas (Online: www.lpi.usra.edu/publications/abtracts.shtml#1psc1134.pdf, last accessed March 29, 2007).

Arp, G., Theil, V., Reimer, A., Michaelis, W., and Reitner, J. 1999. Biofilm exopolymers control microbialite formation at thermal springs discharging into the alkaline Pyramid Lake, Nevada, USA. Sedimentary Geology, **126**: 159–176.

Arp, G., Reimer, A., and Reitner, J. 2001. Photosynthesis-induced biofilms, calcification, and calcium concentrations in Phanerozoic oceans. Science, **292**: 1701–1704.

Aruguete, D.M., Aldstadt, J.H. III, and Mueller, G.M. 1998. Accumulation of several heavy metals and lanthanides in mushrooms (Agaricales) from the Chicago region. The Science of the Total Environment, **224**: 43–56.

Bala, H., Fu, W., Zhae, J., Ding, X., Jiang, Y., Yu, K., and Wang, X. 2005. Preparation of $BaSO_4$ nanoparticles with self-dispersing properties. Colloids and Surfaces A, **252**:129–134.

Baldi, F., Pepi, M., Burrini, D., Kniewald, G., Scali, D., and Lanciotti, E. 1996. Dissolution of barium from barite in sewage sludges and cultures of *Desulfobibrio desulfuricans*. Applied and Environmental Microbiology, **62**: 2398–2404.

Bertram, M.A., and Cowen, J.P. 1997. Morphological and compositional evidence for biotic precipitation of marine barite. Journal of Marine Research, **55**: 677–693.

Bolze, C.E., Malone, P.G., and Smith, M.J. 1974. Microbial mobilization of barite. Chemical Geology, **13**: 141–143.

Bonny, S., and Jones, B. 2003. Microbes and mineral precipitation, Miette Hot Spring, Jasper National Park, Alberta, Canada. Canadian Journal of Earth Sciences, **40**:1483–1500.

Braithewaite, A., and Whitton, B.A.. 1987. Gypsum and halite associated with the cyanobacterium *Entophysalis*. Geomicrobiological Journal, **5**: 43–55.

Buick, R., Dunlop, J.S.R., and Grooves, D.I. 1981. Stromatolite recognition in ancient rocks: an appraisal of irregularly laminated structures in an Early Archaean chert–barite unit from North Pole, Western Australia. Alcheringa, **5**: 161–181.

Brigmon, R.L., Martin, H.W., Morris, T.L., Bitton, G., and Zam, S.G. 1994. Biogeochemical ecology of *Thiothrix* spp. in underwater limestone caves. Geomicrobiology Journal, **12**:141–159.

Burhan, R.Y.P., Trendel, J.M., Adam, P., Wehrung, P., Albrecht, P., and Nissenbaum, A. 2002. Fossil bacterial ecosystem at methane seeps; origin of organic matter from Be'eri sulfur deposit, Israel. Geochimica et Cosmochimica Acta, **66**: 4085–4101.

Cadigan, R.A., and Felmlee, J.K. 1977. Radioactive springs geochemical data related to uranium exploration. Journal of Geochemical Exploration, **8**: 381–395.

Canfield, D.E. 2001. Isotope fractionation by natural populations of sulfate-reducing bacteria. Geochimica et Cosmochimica Acta, **65**: 1117–1124.

Carroue, J-P. 1996. Une presentation originale de la barytine ou des stromatolithes de poids. Mineraux et Fossiles, **246**: 21–22.

Cecile, M.P. 2000. Geology of the northeastern Niddery Lake map area, east-central Yukon and adjacent Northwest Territories. Geological Survey of Canada, Bulletin 553.

Cecile, M.P., Goodfellow, W.D., Jones, L.D., Krouse, H.R., and Shakur, M.A. 1984. Origin of radioactive barite sinter, Flybye springs, Northwest Territories, Canada. Canadian Journal of Earth Sciences, **21**: 383–395.

Cormack, K., Todd, R.L., and Mond, C.D. 1975. Patterns of basidiomycete nutrient accumulation in conifer and deciduous forest litter. Soil Biology and Biochemistry, **106**: 545–554.

Desideri, D., Feduzi, L., Meli, A.A., and Roselli, C. 2006. Leachability of naturally occurring radioactive materials. Journal of Radioanalytical and Nuclear Chemistry, **267**: 551–555.

Dominguez-Rosado, E., Pichtel, J., and Coughlin, M. 2004. Phytoremediation of soil contaminated with used motor oil: I. Enhanced microbial activities from laboratory and growth chamber studies. Environmental Engineering Sciences, **21**: 157–168.

Douglas, S., and Douglas, D.D. 2000. Environmental scanning electron microscopy studies of colloidal sulfur deposition in a natural

microbial community from a cold sulfide spring near Ancaster, Ontario, Canada. Geomicrobiology Journal, **17**: 275–289.

Douglas, S., and Douglas, D.D. 2001. Structural and geomicrobiological characteristics of a microbial community form a cold sulfide spring. Geomicrobiology Journal, **18**: 201–422.

Fortin, D., Ferris, F.G., and Scott, S.D. 1998. Formation of Fe-silicates and Fe-oxides on bacterial surfaces in samples collected near hydrothermal vents on the Southern Explorer Ridge in the northeast Pacific Ocean. American Mineralogist, **83**: 1399–1408.

Gadd, G.M. 1993. Interactions of fungi with toxic metals. New Phytologist, **124**: 25–60.

Ganeshram, R.S., Francois, R., Commeau, J., and Brown-Leger, L. 2003. An experimental investigation of barite formation in seawater. Geochimica et Cosmochimica Acta, **67**: 2599–2605.

Garcia-Pichel, F., and Castenholz, R.W. 1990. Comparative anoxygenic photosynthetic capacity in 7 strains of a thermophilic cyanobacterium. Archives of Microbiology, **153**: 344–355.

Glamoclija, M., Garrel, L., Berthon, J., and Lopez-Garcia, P. 2004. Biosignatures and bacteria diversity in hydrothermal deposits of Solfatara Crater, Italy. Geomicrobiology Journal, **21**: 529–541.

González-Muñoz, M.T., Fernandez-Luque, B., Martínez-Ruiz, F., Chekroun, K.B., Arias, J.M., Rodríguez-Gallego, M., Martínez-Cañamero, M., de Linares, C., and A. Paytan. 2003. Precipitation of barite by *Myxococcus xanthus*: Possible implications for the biogeochemical cycle of barium. Applied and Environmental Microbiology, **69**: 5722–5725.

Greinert, J., Bollwerk, S.M., Derkachev, A., Bohrmann, G., and Suess, E. 2002. Massive barite deposits and carbonate mineralization in the Derugin Basin, Sea of Okhotsk: Precipitation processes at cold seep sites. Earth and Planetary Science Letters, **203**: 165–180.

Grupe, G., and Herrmann, B. 1988. Trace elements in environmental history. Springer-Verlag, New York, N.Y.

Jackson, C.R., Langner, H., Danohoe-Christiansen, J., Inskeep, W.P., and McDermott, T.R. 2001. Molecular analysis of microbial community structure in an arsenite-oxidizing acidic thermal spring. Environmental Microbiology, **3**: 532–542.

Jewell, P.W. 2000. Bedded barite in the geologic record. Special Publication – Society for Sedimentary Geology, **66**: 147–161.

Jones, B., Renaut, R.W., and Rosen, M.R. 2000. Trigonal dendritic calcite crystals forming from hot spring waters at Waikite, North Island, New Zealand. Journal of Sedimentary Research, **70**: 56–603.

Jørgensen, B.B., and Des Marais, D.J. 1986. Competition for sulfide among colorless and purple sulfur bacteria in cyanobacterial mats. FEMS Microbial Ecology, **38**: 179–186.

Karnachuk, O.V., Kurochkina, S.Y., and Tuovinen, O.H. 2002. Growth of sulfate-reducing bacteria with solid-phase electron acceptors. Applied Microbiology and Biotechnology, **58**:482–486.

Kaufman, A.J., and Xiao, S. 2003. High CO_2 levels in the Proterozoic atmosphere estimated from analyses of individual microfossils. Nature, **425**: 279–281.

Kharaka, Y.K., Gunter, W.D., Aggarwal, P.K., Perkins, E.H., and DeBraal, J.D., 1988, SOLMINEQ88: A computer program for geochemical modeling of water–rock interactions: U.S. Geological Survey Water Resources Investigation Report, 88-4227, 88 p.

Kiyokawa, S., Ito, T., Ikehara, M., and Kitajima, F. 2006. Middle Archean volcano-hydrothermal sequence: Bacterial microfossil-bearing 3.2 Ga Dixon Island Formation, coastal Pilbara terrane, Australia. Geological Society of America Bulletin, **118**: 3–22.

Knoll, A.H. 1985. Exceptional preservation of photosynthetic organisms in silicified carbonates and silicified peats. Philosophical Transactions of the Royal Society (of London), **311**: 111–122.

Kojima, H., Teske, A., and Fukui, M. 2003. Morphological and phylogenetic characterizations of freshwater *Thioploca* species from Lake Biwa, Japan and Lake Constance, Germany. Applied and Environmental Microbiology, **69**: 390–398.

Konhauser, K.O., Jones, B., Reysenbach, A.-L., and Renaut, R.W. 2003. Hot spring sinters: keys to understanding Earth's earliest life forms. Canadian Journal of Earth Sciences, **40**: 1713–1724.

Larkin, J.M., and Henk, M.C. 1996. Filamentous sulfide-oxidizing bacteria at hydrocarbon seeps of the Gulf of Mexico. Microscopy Research and Technique, **33**: 23–31.

Larkin, J.M., and Strohl, W.R. 1983. *Beggiatoa*, *Thiothrix*, and *Thioploca*. Annual Reviews in Microbiology, **37**: 341–67.

Leadbeater, B.S.C., and Riding, R. 1986. Biomineralization in lower plants and animals. Oxford University Press, New York.

Lindgren, W. 1933. Mineral Deposits. 4th ed. McGraw-Hill Publishers, New York, N.Y.

Lu, Z.C., Liu, C.Q., Liu, J.J., and Wu, F.C. 2004. The bio-barite in witherite deposits from Southern Qinling and its significance. Progress in Natural Science, **14:** 889–895.

Mann, H., and Fyfe, W.S. 1984. An experimental study of algal uptake of U, Ba, V, Co, and Ni from dilute solutions. Chemical Geology, **44**: 385–398.

Mas, J., and van Gemerden, H. 1987. Influence of sulfur accumulation and composition of sulfur globule on cell volume and buoyant density of *Chromatium vinosum*. Archives of Microbiology, **146**: 362–369.

Merz-Preiss, M. 2000. Calcification in cyanobacteria. *In* Microbial sediments. *Edited by* R.E. Riding and S.M. Awramik. Springer-Verlag, Heidelberg, Germany, pp. 50–56.

Mukherjee, P., Ahmad, A., Mandal, D., Senapati, S., Sinkar, S.R., Khan, M.I., Ramani, R., Parischa, R., Ajayakumar, P.V., Alam, M., Sastry, M., and Kumar, R. 2001. Bioreduction of $AuCl_4^-$ ions by the fungus *Verticillium* sp., and surface trapping of the gold nanoparticles formed. Angewandte Chemie International Edition, **40**: 3585–3588.

Natorff, R., Sienko, M., Brzywczy, J., and Paszewski, A. 2003. The *Aspergillus nidulans* metR gene encodes a bZIP protein which activates transcription of sulphur metabolism genes. Molecular Microbiology, **49**: 1081–1094.

Nelson, D.C. 1989. Physiology and biochemistry of filamentous sulfur bacteria. *In* Autotrophic bacteria. *Edited by* H.G. Schlegel and B. Bowien, Science Tech Publishers, Madison, Wis., pp. 219–238.

Oehler, J.H., and Schopf, J.W. 1971. Artificial microfossils: Experimental studies of permineralization of blue–green algae in silica. Science, **174**: 1229–1231.

Ohno, M., and Tazaki, K. 2000. Biomineralization in biomats at Hirayu Hot Springs. Earth Science, **54**: 298–309.

Orberger, B., Gallien, J.-P., Pinti, D.L., Failin, M., Daudin, L., Grocke, D.R., and Pasava, J. 2005. Nitrogen and carbon partitioning in diagenetic and hydrothermal minerals from Paleozoic black shales, (Selwyn Basin, Yukon Territories, Canada). Chemical Geology, **218**, 249–264.

Overmann, J., and Pfennig, N. 1992. Continuous chemotropic growth and respiration of *Chromatiaceae* species at low oxygen concentrations. Archives of Microbiology, **158**: 59–67.

Palinska, K.A., and Krumbein, W.E. 2000. Perforation patterns in the peptidoglycan wall of filamentous cyanobacteria. Journal of Phycology, **36**: 139–145.

Pasteris, J.D., Freeman, J.J., Goffredi, S.K., and Buck, K.R. 2001. Raman spectroscopic and laser scanning confocal microscopic analysis of sulfur in living sulfur-precipitating marine bacteria. Chemical Geology, **180**: 3–18.

Patritskaya, V., Grabovich, M., Muntyan, M.S., and Dubinina, G.A. 2001. Lithoautotrophic growth of the freshwater colorless

sulfur bacterium *Beggiatoa "leptomitiformis"* D-402. Microbiology, **70**: 14–150.

Pattaragulwanit, K., Brune, D.C., Trüper, H.G., and Dahl, C. 1998. Molecular genetic evidence for extracytoplasmic localization of sulfur globules in *Chromatium vinosum*. Archives of Microbiology, **169**: 434–444.

Prange, R.C., Chauvistre, R., Modrow, J., Hormes, J., Trüper, H.G., and Dahl, C. 2002. Quantitative speciation of sulfur in bacterial sulfur globules: X-ray adsorption spectroscopy reveals at least three different species of sulfur. Microbiology, **148**: 267–276.

Radanovic-Guzvica, B. 1999. The average structural density of barite crystals of different habit types. Geologia Croatica, **52**: 59–65.

Rajashekhar, M., and Kaveriappa, K.M. 2003. Diversity of aquatic hyphomycetes in the aquatic ecosystem of the Western Ghats of India. Hydrobiologica, **501**: 167–177.

Reichenback, H. 1981. The taxonomy of the gliding bacteria. Annual Reviews in Microbiology, **35**: 339–364.

Reinartz, M., Tschape, J., Bruser, T., Trüper, H.B., and Dahl, C. 1998. Sulfide oxidation in the phototrophic sulfur bacterium *Chromatium vinosum*. Archives of Microbiology, **170**: 59–68.

Riding, R.E., and Awramik, S.M. 2000. Microbial Sediments. Springer, New York, N.Y.

Rippka, R., Deruelles, J., Waterbury, J.B., Herdman, M., and Stanier, R.Y. 1979. Generic assignments, strain histories and properties of pure cultures of cyanobacteria. Journal of General Microbiology, **111**: 1–16.

Sakorn, P., Rakariyatham, N., Niamsup, H., and Nongkunsarn, P. 2002. Rapid detection of myrosinase-producing fungi: a plate method based on opaque barium sulphate formation. World Journal of Microbiology and Biotechnology, **18**: 73–74.

Sanchez-Moral, S., Luque, L., and Canaveras, J.C. 2004. Bioinduced barium precipitation in St. Callixtus and Domitilla catacombs. Annals of Microbiology, **54**: 1–12.

Sasaki, N., and Minato, H. 1982. Relationship between lattice constants and strontium and calcium contents of hokutolite. Mineralogical Journal, **11**: 62–71.

Schlegel, H.G., and Bowien, B. 1989. Autotrophic Bacteria. Science Tech Publishers, Madison, Wisconsin.

Schultze-Lam, S., and Beveridge, T.J. 1994. Nucleation of celestite and strontianite on a cyanobacterial S-layer. Applied and Environmental Microbiology, **60**: 447–453.

Senko, J.M., Campbell, B.S., Henriksen, J.R., Elshahed, M.S., Dewers, T.A., and Krumholz, L.R. 2004. Barite deposition resulting from phototrophic sulfide-oxidizing bacterial activity. Geochimica et Cosmochimica Acta, **68**: 773–780.

Sermon, P.A., McLellan, N.M., and Collins, I.R. 2004. Formation of $BaSO_4$ nanoribbons from a molecular mangle. Crystal Engineering Communications, **6**: 469–473.

Shen, Y., Buick, R., and Canfield, D.E. 2001. Isotopic evidence for microbial sulphate reduction in the early Achaean era. Nature, **410**: 77–81.

Shikazono, N. 1994. Precipitation mechanisms of barite in sulfate-sulfide deposits in back-arc basins. Geochimica et Cosmochimica Acta, **58**, 2203–2213.

Simonsen, R. 1987. Atlas and catalogues of the diatom types of Freidrich Hustedt, Vol. 2. Atlas, Stuttgart – J. Cramer, Berlin, Germany, pls. 1–139.

Smith, E., Hamilton-Taylor, J., Davison, W., Fullwood, N.J., and McGrath, M. 2004. The effect of humic substances on barite precipitation-dissolution behaviour in natural and synthetic lake waters. Chemical Geology, **207**: 81–89.

SOLMINEQ88. 1988. A computer program for geochemical modeling of water-rock interactions developed by the United States Geological Survey. Water Investigations Report 88-05.

Stark, A.I.R., Wogelius, R.A., Collins, I.R., and Vaughan, D.J. 2004. Kinetic and thermodynamic controls on the precipitation and morphology of barite ($BaSO_4$). *In* Goldschmidt conference proceedings, Copenhagen, Denmark. Theme 2: The dynamic interface. Extended abstract, p. A148.

Steiman, R., Ford, L., Ducros, V., Lafond, J.L., and Guiraud, P. 2004. First survey of fungi in hypersaline soil and water of Mono Lake area (California). Antonie van Leeuwenhoek International Journal of General and Molecular Microbiology, **85**: 69–83.

Steudel, R. 1989. On the nature of the "elemental sulfur" (S^0) produced by sulfur-oxidizing bacteria—a model for S^0 globules. *In* Autotrophic bacteria. *Edited by* H.G. Schlegel and B. Bowien. Science Tech Publishers, Madison, Wis., pp. 289–303.

Su, H.-Y., Lee, J.-S., and Yu, S.-C. 2002. Dopant effect on hokutolite crystals synthesized with hydrothermal process. Western Pacific Earth Sciences, **2**:301–318.

Tazaki, K., and Watanabe, H. 2004. Biomineralization of radioactive sulfide minerals in strong acidic Tamagawa Hot Springs. Science Reports of the Kanazawa University, **49**:1–24.

Tazaki, K., Webster, J., and Fyfe, W.S. 1997. Transformation processes of microbial barite to sediments in Antarctica. Japanese Journal of Geology, **26**: 63–68.

Teske, A., and Nelson, D.C. 2005. The genera *Beggiatoa* and *Thiothrix*. *In* The Prokaryotes—an evolving electronic resource for the microbiological community, Beta Release 3.20. *Edited by* M. Dworkin. (Online: www.springerlink.com/content/r21k000qn714j380/, last updated November 2006).

Tomson, M.B., Kan, A.T., Fu, G., and Al-Thubaiti, M. 2003. NORM scale formation, control, and relation to gas hydrate control. Proceedings of the 10th International Petroleum Environmental Conference (IPEC), Houston, Texas, November 11–14, 2003. Extended abstract, p. 34.

Silica, M.E., Bohrmann, G., Dube, T.E., and Poole, F.G. 2003. Formation of modern and Paleozoic stratiform barite at cold methane seeps on continental margins. Geology, **31**: 897–900.

van Everdingen, R.O. 1972. Thermal and mineral springs in the southern Rocky Mountains of Canada. Water Management Service, Department of the Environment, Water Management Service, Environment Canada.

Vinogradova, Z.A., and Koval'skiy, V.V. 1962. Elemental composition of Black Sea plankton. Doklady Rossiskoj Akademii Nauk. SSSR, **147**: 217–219.

Wagner, T., Kirnbauer, T., Boyce, A.J., and Fallick, A.E. 2005. Barite-pyrite mineralization of the Wiesbaden thermal spring system, Germany: a 500-kyr record of geochemical evolution. Geofluids, **5**:124–139.

Walter, W.R., and Des Marais, D.J. 1993. Preservation of biological information in thermal spring deposits; developing a strategy for the search for fossil life on Mars. Icarus, **101**: 129–143.

Weber, R.W.S. 2002. Vacuoles and the fungal lifestyle. Mycologist, **16**: 10–20.

Westall, F. 1999. The nature of fossil bacteria: A guide to the search for extraterrestrial life. Journal of Geophysical Research, **104**: 16 437 – 16 451.

Wher, J.D., and Sheath, G. 2003. Freshwater algae of North America: Ecology and classification. Academic Press, San Diego, Calif.

Younger, P. 1986. Barite travertine from southwestern Oklahoma and west-central Colorado. Unpublished M.Sc. thesis, Oklahoma State University, Stillwater, Okla., USA.